FORMULATION OF A RIP CURRENT FORECASTING TECHNIQUE THROUGH STATISTICAL ANALYSIS OF RIP CURRENT-RELATED RESCUES

By

JASON A. ENGLE

A THESIS PRESENTED TO THE GRADUATE SCHOOL
OF THE UNIVERSITY OF FLORIDA IN PARTIAL FULFILLMENT
OF THE REQUIREMENTS FOR THE DEGREE OF
MASTER OF SCIENCE

UNIVERSITY OF FLORIDA

2003

This document is dedicated to Molly.

ACKNOWLEDGMENTS

This research was funded by the 2000-2002 and 2002-2004 Florida Sea Grant Program. I appreciate the commitment they made to this project. I thank the Volusia County Beach Patrol for providing the detailed lifeguard rescue logs used in this investigation, for offering valuable insight on rip current activity in its area and for cooperating with field experiments conducted along its beaches. I would also like to thank the United States Army Corps of Engineers for providing the directional wave data that was essential to this research.

I extend my greatest appreciation to my supervisory committee chairman Dr. Robert Thieke. His support and encouragement were unwavering from the beginning when I conducted undergraduate research, to the completion of this thesis. I also thank Jamie MacMahan. His generosity and concern were a vital part of my experience here; he created opportunities to perform fieldwork in numerous locations and gain the practical experience that has opened many doors for me. His input was equally vital to the research presented herein. I also thank Dr. Andrew Kennedy and Dr. Robert G. Dean for always finding time for my questions and serving on my supervisory committee.

Finally, I would like to thank my family; my parents (Molly and Dan Engle) for their unconditional support and encouragement throughout this process (everyone should be so lucky) my brother Ben for showing us around Gainesville when we arrived and patiently commiserating about the stresses of college life. Most of all, I want to thank my

wife Jennifer for being a patient and inspiring partner in this “gradual” school endeavor. We did it!!

TABLE OF CONTENTS

Abstract of Thesis Presented to the Graduate School
of the University of Florida in Partial Fulfillment of the
Requirements for the Degree of Master of Science

FORMULATION OF A RIP CURRENT FORECASTING TECHNIQUE THROUGH STATISTICAL ANALYSIS OF RIP CURRENT-RELATED RESCUES

By

Jason A. Engle

May 2003

Chair: Robert J. Thieke
Major Department: Civil and Coastal Engineering

Lifeguard rescue logs from Daytona Beach, Florida, were examined in an effort to correlate rip current-related rescues with concurrent wave and wind measurements on a barred shoreline with periodically spaced rip channels. The frequency of rip current rescues increased markedly during (1) shore-normal wave incidence, (2) mid-low tidal stages and (3) narrow directional spreading. Correlations with wave direction, and tide stage are based on analysis of eight months of wave data and rescues while the correlation with directional spreading is based on a five-week period for which spectral wave data are available. The National Weather Service's present rip current forecasting technique is modified to include wave direction tidal stage and directional spreading as predictive parameters. The inclusion of these new parameters and the elimination of two wind parameters result in improved overall performance of the predictive index and, specifically, more accurate forecasting of days with a very high number of rip current rescues. While it is recognized that the use of rescue data as a proxy for rip current

measurements is highly imperfect, the vast wealth of rescue data still lends itself well to making statistical inferences; this is particularly true for the influence of the wave direction and tide stage, where the data sets are the largest.

CHAPTER 1
INTRODUCTION

An examination of east-central Florida rip current data was undertaken at University of Florida to correlate rip current-related rescues with concurrent wave and weather conditions. This investigation is one component of an ongoing project at University of Florida, funded by Florida Sea Grant, to formulate a rip current predictive index. Daytona Beach, located in Volusia County, was selected as the focus of this study based on its relatively high number of rip current-related rescues. Volusia County is located 100km southeast of Jacksonville on Florida's Atlantic coast (Figure 1.1) and has 70km of coastline, most of which is sandy beach. In Florida, rip currents cause more deaths per year, on average, than hurricanes, lightning and tornadoes combined and Volusia County records more rip-related rescues than all other Florida counties combined (Lascody 1998). A combination of frequent, strong rip currents and a high volume of beachgoers result in thousands of rescues per year. During 2001, 2399 people were rescued from rip currents, which accounted for 68% of the total rescues on Volusia County beaches (Volusia County 2003). Remarkably, only three drownings occurred in 2001 (all on unguarded beaches), which is a testament to the skill and dedication of the Volusia County Beach Patrol.

The determination of a predictive index for rip currents is vitally important for the protection of human life. Such an index allows governmental agencies to issue rip current warnings directly to the public and allows lifesaving corps to set-up preventative measures according to the magnitude of the rip current threat. The National Weather

Service (NWS) has developed rip current forecasting techniques for the east coast of Florida and issues statements detailing rip current risk through the media, such as National Oceanographic and Atmospheric Administration (NOAA) weather radio.

Figure 1.1: Map of Florida depicting location of study site in Daytona Beach

Lushine (1991) developed the Lushine Rip Current Scale (LURCS) an empirical forecasting technique that utilizes wind direction and velocity; swell height and the time of low tide to forecast rip current danger in South Florida. The LURCS forecasting technique was adapted for use in east central Florida (ECFL LURCS) at which time swell period was included as a factor and the tidal factor was changed. The ECFL LURCS' false alarm ratio indicated that there was room for improvement with the forecasting technique (Lascody 1998).

A statistical analysis of the wind and wave conditions concurrent with rip current rescues on Daytona Beach and New Smyrna Beach Florida is presented. Modifications to the ECFL LURCS forecasting technique are introduced and the performance of the original scale is compared with that of the modified version. The new predictive factors include 1) an improved tide factor, 2) a wave direction factor, and 3) a directional

spreading factor. The inclusion of these new factors and the elimination of two wind factors improve the accuracy of the ECFL LURCS scale in Volusia County.

Past research into the characteristics of rip currents and the mechanisms that affect their intensity are outlined in Chapter 2. The LURCS and ECFL LURCS rip current forecasting techniques are outlined in chapter 3, along with the scientific rationale for the improvements made to the techniques. The data sources for this investigation are detailed in chapter 4 and the analyses of these data are presented in chapter 5. Changes made to the rip current index are presented and the performance of the new scale is evaluated in chapter 6. Finally, Chapter 7 outlines the implications of this study on future work and the conclusions are presented in Chapter 8.

CHAPTER 2
RIP CURRENT CHARACTERISTICS

Rip currents are narrow, strong currents that move seaward through the surf zone (Bowen 1969). Rip currents may occur at specific locations due to interaction with shore structures such as jetties, piers and groins or due to the geometry of the shoreline such as on a beach between headlands, however rip currents also occur along straight beaches. Nearshore currents may (simplistically) be considered bounded by two limiting cases. The first is a longshore current driven by waves breaking at oblique angles to the shore. The second case is a nearshore cell circulation, depicted in Figure 2.1, resulting from shore-normal waves. Commonly, conditions fall between these two cases and both a net longshore current and cell circulation occur simultaneously (Komar 1976).

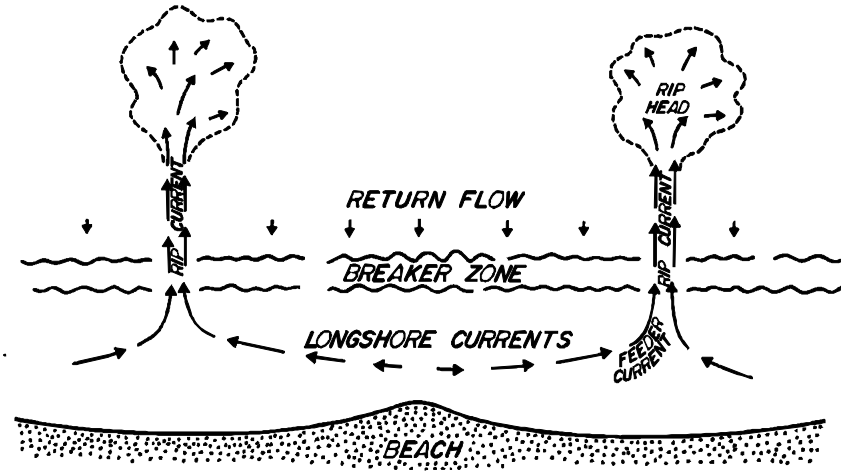

Figure 2.1: Schematic of a simplified nearshore cell circulation system (from Komar 1976).

Shepard et al. (1941) were among the first to qualitatively describe the features and behavior of rip currents in a scientific manner. They observed that the intensity and

distance that the rip currents travel from shore were related to the height of the incident waves. Subsequent study by Shepard and Inman (1950) showed that rip currents are one part of a nearshore circulation system. This system, illustrated in Figure 2.1, consists of the diffuse shoreward transport of water due to breaking waves, the longshore transport of water in feeder currents between the shore and bar and strong, narrow seaward-directed rip currents in the rip channels. Shepard and his colleagues also reasoned that a longshore variation of incident wave height was the forcing mechanism for the development of such a circulation system.

McKenzie (1958) observed rip currents in New South Wales, Australia over a six-year period and made qualitative descriptions of rip currents. Wave direction and tidal stage were observed to affect the rip current systems: high waves and low tide strengthened the rip currents and acute wave angles to the shore created strong longshore currents and rip currents that turned obliquely seaward.

Researchers, up to that point in time, had observed rip current behavior and attributed the source of nearshore cell circulation to mass-transport of water shoreward over the bar due waves, and a corresponding seaward return flow in the form of rip currents. The ability of researchers to model near-shore circulation was greatly improved when Longuet-Higgins and Stewart (1964) introduced the concept of radiation stress and described the change in mean sea level resulting from waves that encounter a sloping bottom. Increases in the mean sea level (set-up) occur shoreward of the breaker-line and a decrease of mean sea level (set-down) occurs at the break point. Radiation stress is the excess flow of momentum due to the presence of waves. This stress induces a gradient in the mean water level that balances the gradient of the radiation stress: the sea surface

becomes inclined away from shore so that the maximum set-up occurs at the beach. The resulting hydraulic head is directed away from shore, providing an energy source in the cross-shore. This discovery clarified that the forcing mechanisms of rip currents most likely includes both radiation stress and mass-transport of water into the surf-zone.

Bowen (1969) confirmed, theoretically, that high waves, so long as they break continuously from the break point to the beach, would cause a greater setup than lower waves. This is principally due to (1) the fact that a higher wave will break further from shore, initiating the sea-surface gradient at a position that is further seaward than a lower wave and (2) the setup is proportional to wave height.

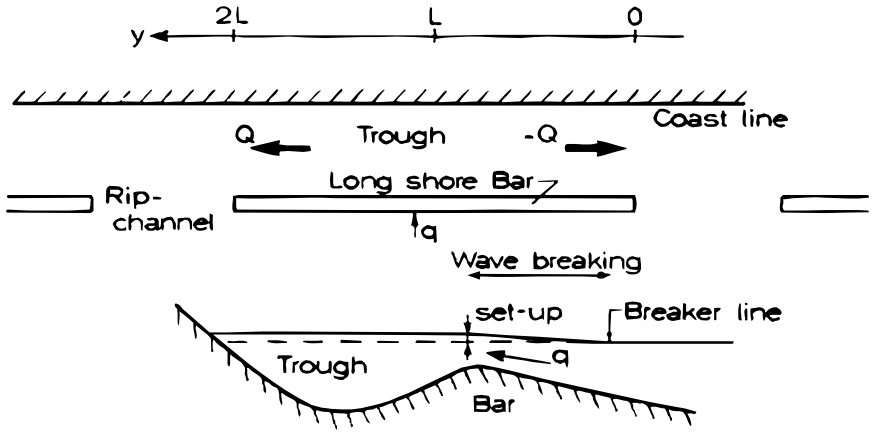

Figure 2.2: Sketch of an alternating bar and rip channel system and setup due to wave breaking (from Fredsoe 1992).

A longshore variation of breaking wave height will cause a variation in wave set up along the shore and a longshore pressure gradient develops (Bowen 1969, Dalrymple 1978, Haller et al. 1997). Feeder currents will flow away from zones of high waves and toward zones of low waves where they converge and move seaward as rip currents. Laboratory experiments conducted by Haller et al. (1997) confirmed that rip channels through an otherwise longshore uniform bar induce longshore pressure gradients and cell circulations in the nearshore. Wave heights were actually higher in the rip channel than

over the bar due to interaction with the rip currents and the deeper bathymetry of the rip channel; however, the waves would break very close to shore in the rip channels, which reduced setup significantly. The longshore variation of setup was, thus, still highest shoreward of the bar and lowest in the rip channel. The longshore pressure gradient between the shore and bar still drives flows toward the rip channels where they converge and move seaward.

Rip currents in nature are often observed in combination with three-dimensional surf-zone morphology. Several specific types have been described in the literature, but all are variations of on one theme: longshore variation of bottom contours in the nearshore, where rip currents occur in the deeper portions and diffuse shoreward transport occurs over the shallower regions. Analytical solutions developed by Mei and Liu (1977) described the effects of longshore varying surf zone bathymetry on longshore pressure gradients. 3-dimensional bar and rip channel bathymetry were found to induce pressure gradients laterally toward the rip channel inshore of the bar. Oh and Dean (1996) conducted laboratory experiments, which showed that rip currents are stable on three-dimensional, barred beaches and confirmed that mass transport is shoreward over the bar and seaward in the rip channels. The beaches of Volusia County, the site for this investigation, are straight with longshore-alternating bars and rip channels (Figure 2.2).

The factors that modulate the strength of rip currents with a bar and rip channel morphology have been investigated in the laboratory and, to a limited extent, in the field. Sonu (1972) observed modulations in rip current intensity corresponding to tidal stage and incident wave direction in field experiments conducted in Florida's panhandle at Seagrove Beach. His measurements revealed increased rip current intensity during low

tide. The tidal level was thought to be significant due to both the confinement of rips to narrower regions in the surf zone and due to stronger wave breaking at the bar during low tide. Cell circulation was observed only during shore-normal wave incident angles and a meandering longshore current was dominant during oblique wave incidence. Although the rip current measurements were relatively short in duration, significant pulsations were observed at the wave-group frequencies. It was postulated that the pulsations could be the result of infragravity motions in the surf-zone. Dronen et al. (2002) conducted experiments in a wave basin with a bar and single rip channel. Cell circulation consisting of strong, narrow rip current flow and weaker return flow over the bar was observed. A series of test runs was performed with varying wave height and water level and revealed that rip current velocity increased with increasing wave height and decreasing water level. Brander (1999) and Brander and Short (2001) conducted field experiments at Palm Beach, NSW, Australia to investigate low-energy rip current systems. Rip flow was modulated by the tide, reaching maximum velocity at low tide and minimum velocity at high tide. Pulsations in rip flow were observed at 0.0078 Hz (128 s.). The pulsations lasted for several minutes and resulted in fluctuations of $\forall$ 0.4 m/s. No wave measurements were taken during the experiment, and the forcing mechanisms for the modulation of the mean flow and the pulsations were not investigated. The author had an opportunity to participate in the Naval Postgraduate School's RIP current EXperiment (RIPEX) in Monterey, CA spring of 2001. Rip current pulsations occurred on infragravity time scales (0.004—0.04 Hz). The pulsations were attributed to cross-shore infragravity motions of long waves, which increase shoreward and with increasing wave height

(MacMahan et al. 2003). In this investigation, rescue data are utilized in an effort to detect whether dangerous rip current pulsations are present.

MacMahan et al. (2000) utilized video imagery from the U. S. Army Corps of Engineers Field Research Facility in Duck, NC to illustrate the relict nature of bar and channel configurations. It was found that a particular bar-and-channel system can persist for weeks or months until they are reconfigured by storm events and that rip channels form again as soon as the storms subside. Rip current-related rescues occur in Volusia County 65% of the days from May through August when the waters are warm enough for significant numbers of people to enter the surf. This fact suggests that rip currents are present nearly all of the time. Anecdotal evidence from the Volusia Beach Patrol supports this assertion and that some of the rip currents are stationary for days or weeks.

In summary, the principal factors affecting rip current strength, as documented in the literature, are 1) Wave height (most researchers), 2) Wave direction (Sonu 1972), and 3) Tidal Stage (McKenzie 1958, Sonu 1972, Brander 1999, Brander and Short 2001, and Dronen et al. 2002). Rip current pulsations were observed by Sonu (1972), Brander and Short (2001) and MacMahan et al. (2003). These phenomena were attributed to wave energy in the infragravity frequency band by Sonu (1972) and MacMahan et al. (2003) showed an that interaction of long waves in the surf-zone force pulsations. Rip currents are persistent and relict (MacMahan 2000), which may explain the high numbers of rescues that occur regularly along Florida's Atlantic coast. This study's goal was to investigate correlations between wave parameters, tide and rip current rescues on Daytona Beach, Florida and to use this information to improve the empirical rip current forecasting technique employed by the National Weather Service.

CHAPTER 3
RIP CURRENT FORECASTING

The ephemeral nature of rip currents complicates possible efforts to directly detect them and such an installation in the rough environs of the surf zone requires constant maintenance. For these reasons, few data records exist to document the activity and strength of rip currents in the field. Rip current rescue records provide a long-term, quantitative (although less precise) measure of rip activity and are available for many guarded beaches. The LURCS and ECFL LURCS scales presently in use were formulated by comparing rip current rescues and drownings in concert with the concurrent wind and sea state. The ECFL LURCS scale forecasts rip current threat based on four parameters including wind speed, wind direction, swell height and swell period. These scales' performance in NWS severe weather warning verification tests (Lascody 1998) indicate the viability of rescue data in the detection of rip currents. Rip rescue records were used in this investigation as markers for the existence of rip currents at the time of the rescue.

Lascody (1998) noted that Volusia County Florida accounts for a disproportionate number of rip-related rescues and drownings in Florida each year as a result of both its popularity with beachgoers and features that encourage the formation of rip currents. The high frequency of rescues in Volusia County makes it a favorable location to utilize statistical techniques with rip current-related rescues as a gauge of rip occurrence. Figure 3.1 depicts the number of rip current rescues in the study area per day during the calendar year 1996. From this plot it is evident that rip current are present most days (during the

warm summer months) and that, presumably, the strength of the rip currents varies considerably day to day.

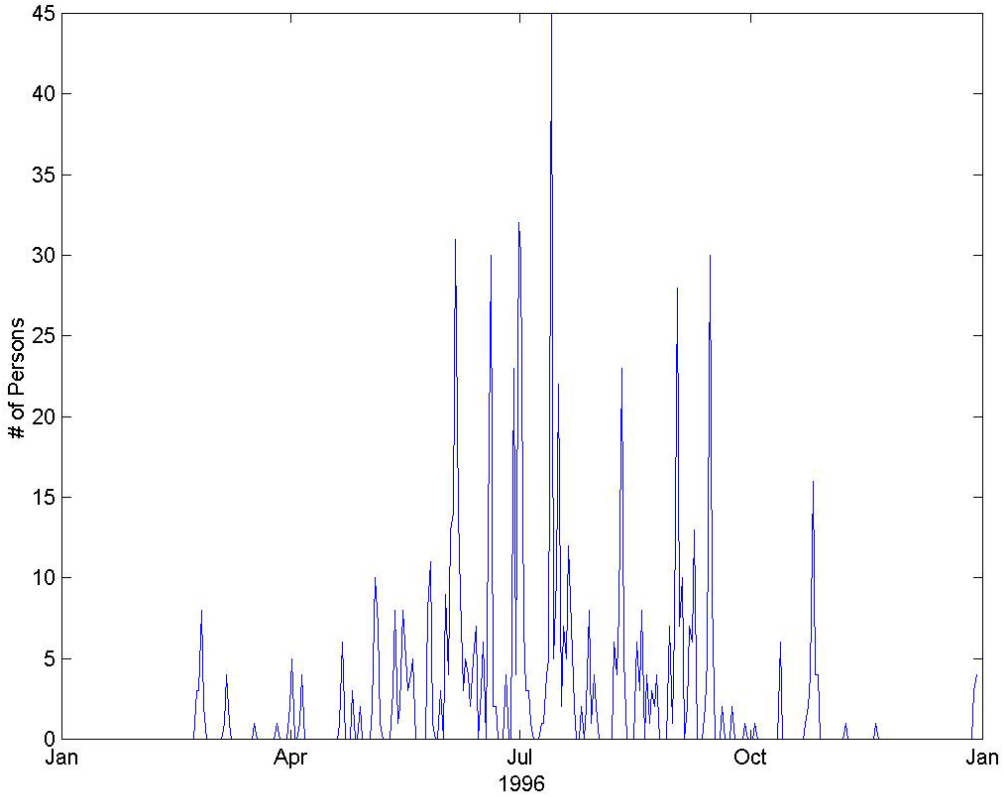

Figure 3.1: Number of persons rescued per day on Daytona Beach and New Smyrna Beach for calendar year 1996. The majority of rescues occurred from May through September, corresponding to the months of greatest beach attendance.

Lushine (1991) showed that 74% of the likely rip current drownings in southeast Florida occurred in the six-hour period from two hours before to four hours after low tide. Sonu (1972), Brander (1999) and others showed that flow velocity in rip channels is tidally modulated with velocity increasing towards low tide and anecdotal evidence from Volusia County lifeguards supported this association. This investigation was initiated with the expectation that a relationship would exist between lower mean water levels and increased rip current rescues. The ECFL LURCS scale includes a single adjustment for

times of high astronomical tides, but does not account for the tidal stage when forecasting rip current threat.

Sonu (1972) observed that near shore circulations occurred under the action of shore-normal wave incidence and that a longshore current dominated under oblique-wave incidence. The NOAA buoys near east central Florida, unfortunately, do not measure wave direction and thus the ECFL LURCS index, which relies on offshore buoys for its wave data, does not include it as a factor. The University of Florida investigation was initiated on the assumption that wave direction could be an important parameter in the prediction of rip currents. The forcing mechanism of cell circulation (the onshore flux of the onshore component of momentum) is maximized during shore-normal waves, presumably causing stronger rip currents.

The energy contained in an incident wave field is spread over a range of directions about a mean. Directional spreading describes the characteristic width of that range. Narrow directional spreading would result in a greater flux of momentum in the mean direction than would a wider spreading (which would direct a greater proportion at angles away from the mean) and, in the case of relatively shore-normal mean direction, would cause stronger rip currents. It was hypothesized that a linkage would exist between narrow directional spreading and higher rip current rescue frequency.

Rip current pulsations were observed qualitatively by Shepard (1950) and were observed to occur roughly on the time scale of wave ‘sets’ or groups of higher waves. Past research in the field (Sonu 1972, MacMahan et al. 2003) and laboratory (Haller et. al. 1997) noted the same modulation of rip currents in their velocity records. These changes may occur rapidly and during these conditions a swimmer could unknowingly

move into a rip or feeder channel at a time of low rip velocity, be surprised by a sudden pulse and be swept into the neck of the rip current. It is even possible that such unsteady behavior could pose an even greater threat to public safety than the mean current itself. For these reasons it was thought that a relationship would exist between rip current frequency and the relative strength of the wave groups, and that some measure of the potential unsteadiness of the rips would be helpful in the prediction of the threat.

CHAPTER 4
DATA

Site Description

The study site, including Daytona Beach and New Smyrna Beach, was 22.5km in length (Figure 4.1). The coastline in this region is straight with sandy beaches. The average beach slope from the upper beach face to depth of closure is 1/45 and the mean sediment diameter is 0.20mm at the shoreline (Charles et al. 1994). Offshore contours are approximately shore-parallel and the bottom slope is relatively mild out to the continental shelf, which is 70km from shore. Average deep-water wave height (for calendar year 1996) at the site was 0.7m and storm-generated waves were frequently 1.5m or more. Tides are semidiurnal with a maximum range of approximately 2m. Incident wave directions are highly variable throughout the year and tend to be from the north during the winter and from the south during the summer. The nearshore bathymetry is characterized as an alternating bar and rip channel morphology.

Rip Current Rescue Data

Beach rescue data were acquired from Volusia County Beach Patrol rescue logs. Lifeguard personnel recorded every rescue event with the time of day, location, number of victims, and type of rescue (animal bite, rip current, etc); an example rescue log is presented in Figure 4.2. Only the rip current-related rescues are considered in this investigation. Volusia County's beaches are subdivided into six zones. Only three of the zones' records are available for 1996 including those of Daytona Beach and New Smyrna Beach; only those three are used in this study.

Buoy Wind Data

The original ECFL LURCS scale received all of its wind input data from NOAA National Data Buoy Center (NDBC) Station 41009 archives. Buoy 41009 is located 37 kilometers east of Cape Canaveral Florida in 42 meters water depth. Wind speed and wind direction were averaged over an eight-minute period and recorded on the hour. (NDBC 1996).

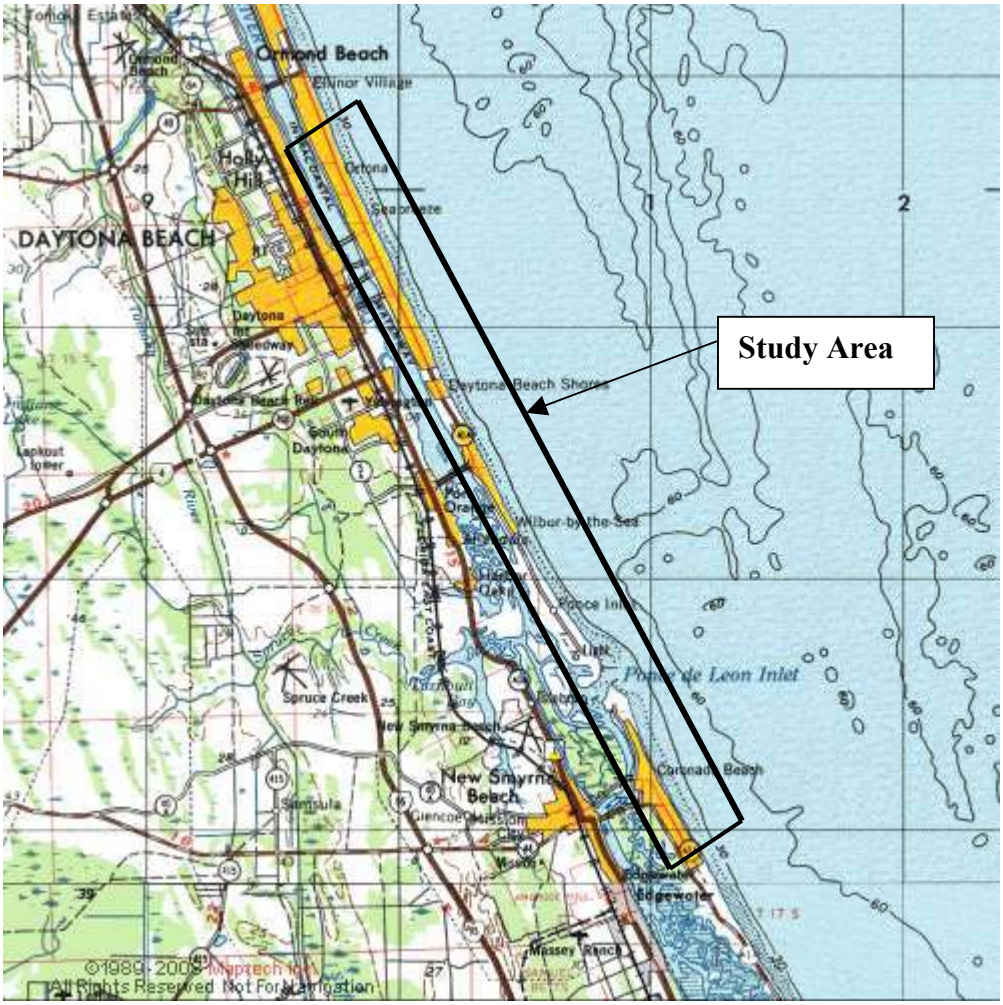

Figure 4.1: Map of study site in Volusia County, FL. Daytona Beach is at the northern end, Ponce de Leon Inlet is in the southern portion and New Smyrna Beach is at the southern end of the study area

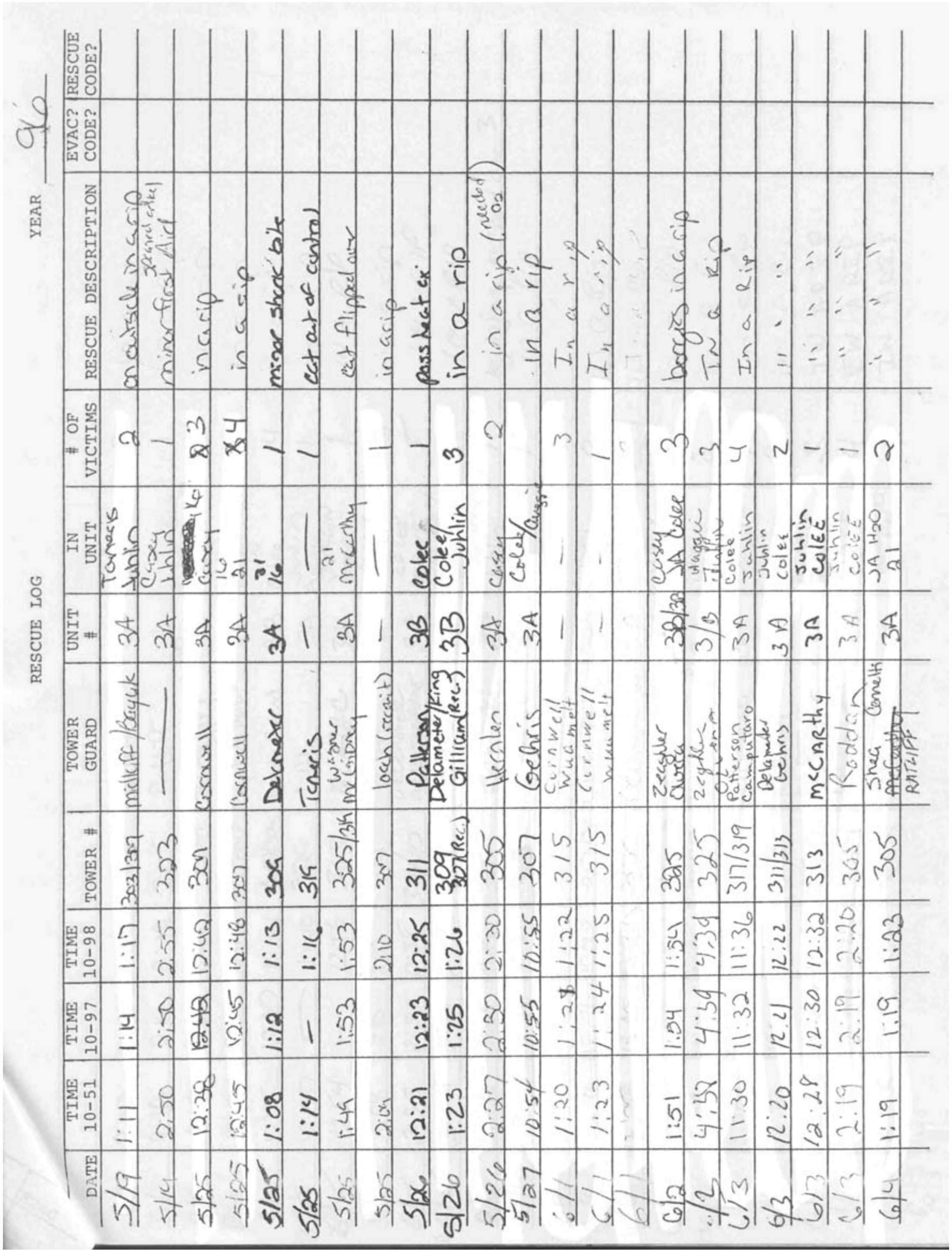

RESCUE LOG — YEAR 96

DATE	TIME 10-51	TIME 10-97	TIME 10-98	TOWER #	TOWER GUARD	UNIT #	IN UNIT	# OF VICTIMS	RESCUE DESCRIPTION	EVAC? CODE?	RESCUE CODE?
5/19	1:11	1:14	1:17	303/307	Mellott/Bayuk	3A	Tomecis Juhlin	2	on outside in a rip		
5/19	2:50	2:50	2:55	303	—	3A	Casey Juhlin	1	minor first aid (scraped ankle)		
5/25	12:38	12:43	12:49	301	Cornwell	3A	Casey	2 3	in a rip		
5/25	12:45	12:45	12:48	301	Cornwell	3A	16 21	3 4	in a rip		
5/25	1:08	1:12	1:13	305	Delmonte	3A	21 16	1	minor shark bite		
5/25	1:14	—	1:16	316	Tomecis	—	—	1	got out of control		
5/25	1:49	1:53	1:53	325/316	Wagner McCarthy	3A	21 McCarthy		got flipped over		
5/25	2:04		2:10	307	Loch (recruit)	—	—	1	in a rip		
5/26	12:21	12:23	12:25	311	Patterson	3B	Colee	1	pass hat ck		
5/26	1:23	1:25	1:26	309 307 (Rec.)	Delamente/King Gilliam (Rec.)	3B	Colee/Juhlin	3	in a rip		
5/26	2:27	2:30	2:30	305	Hensler	3A	Casey	2	in a rip (needed O2)		
5/27	10:54	10:55	10:55	307	Gehris	3A	Colee/Casey		in a rip		
6/1	1:20	1:28	1:22	315	Cornwell Wuchmelt	—	—	3	In a rip		
6/1	1:23	1:24	1:25	315	Cornwell Wuchmelt	—	—	1	In a rip		
6/1											
6/2	1:51	1:54	1:54	305	Zeigler Christie	3B/3A	Casey JA Colee	3	boogies in a rip		
6/2	4:32	4:34	4:34	325	Zeigler [illegible]	3/B	Maggie Juhlin	3	In a rip		
6/3	11:30	11:32	11:36	317/319	Patterson Campulato	3A	Colee Juhlin	4	In a rip		
6/3	12:20	12:21	12:22	311/313	Delamente Gehris	3A	Juhlin Colee	2	" "		
6/3	12:29	12:30	12:32	313	McCarthy	3A	Juhlin Colee	1	" "		
6/3	2:19	2:19	2:20	305	Roddan Cornelli	3A	Juhlin Colee	1	" "		
6/4	1:19	1:19	1:23	305	Shea McCarthy Ratliff	3A	JA H2O 21	2	" "		

Figure 4.2: Example rescue log from Volusia County Beach Patrol. Only entries with 'rip' mentioned explicitly in the rescue description were used in this investigation.

Directional Wave Data

Archived directional wave data and mean water level (tide) data are not available from NOAA NDBC buoys in the vicinity of east central Florida, so directional wave and water level data were obtained from the U.S. Army Corps of Engineers Waterways Experiment Station (WES). A field measurement effort at Ponce de Leon Inlet was conducted by WES from October 1995 to November 1997 to acquire tidal inlet physical processes data (USACE 1995). Three directional wave gages were deployed in the waters adjacent to the inlet (Figure 4.3); two were utilized in this investigation: one designated DWG1EBB1 (EBB) located on the ebb shoal 1200m from shore in 7 meters water depth and a second designated DWG1INT1 (INT) located 4 kilometers north of the inlet and 1.5 kilometers from shore in 14 meters water depth. The INT gage was near the center of the study site. The wave gages consisted of three pressure sensors in an equilateral, triangular layout 1.4m on a side with a known compass orientation at the time of deployment. Both wave gages sampled at 5 Hz continuously. All wave parameters, with the exception of wave groupiness, were taken from the INT gage to eliminate any possible effects of the inlet on the wave data.

Directional wave and water level statistics computed by WES, and available at the WES website, were used in the long-term portion of this investigation including 1) significant wave height, 2) peak wave period, 3) peak wave direction, and 4) mean water level; Table 4.1 is an example of the data. Each statistic was reported hourly. Tidal stages were calculated from the height of water at the wave gage after subtracting the mean water level. For coherence, wind and wave direction were transformed so that zero degrees corresponds with a shore-normal, onshore orientation and positive angles are

Figure 4.3: Map of U.S. Army Corps of Engineers wave gages deployed at Ponce Inlet, FL (from USACE 1995).

Table 4.1: Example of USACE WES directional wave data. Wave direction was subsequently transformed so that zero degrees corresponded to shore-normal wave incidence (azimuth of shoreline = 62°).

Mo.	Day	Yr.	Time (UTM)	Wave Height (m)	Dom. Wave Period (s)	Wave Dir. Azimuth (deg.)	Mean Water Level (m)
6	1	96	0	1.97	5.8	60	15.7
6	1	96	100	2.07	5.8	57	15.5
6	1	96	200	1.95	9.1	48	15.2
6	1	96	300	1.88	6.1	56	14.8
6	1	96	400	1.92	7.5	57	14.4
6	1	96	500	1.85	6.7	65	14.2
6	1	96	600	1.89	7.5	60	14.1
6	1	96	700	1.8	7.1	63	14.2
6	1	96	800	1.72	7.1	64	14.5
6	1	96	900	1.63	8	58	14.8
6	1	96	1000	1.67	8	56	15.1
6	1	96	1100	1.57	7.1	62	15.3

counter-clockwise from shore-normal. These wave data were the input for both the ECFL LURCS index and the modified index. All of the wind, wave and rip rescue data were limited to the same 11 am to 5pm time of interest to reflect the hours of peak beach attendance, based on rip current rescue records.

Directional Spectral Estimation

The second phase of the investigation required the estimation of the wave spectra and the calculation of a wave groupiness parameter, both of which required analysis of the original time series data. WES made time series from the INT and EBB wave gages available to the University of Florida for the period from May 27th to July 6th, 1996. WES retrieved this 5-week period of the time series data from archived magnetic tape before an equipment failure that prevented further data recovery.

Time series from the three-pressure sensor arrays were divided into one-hour increments. Hourly records with less than 2^{14} samples, corresponding to a 54-minute record length at 5 Hz, were eliminated to maximize the spectral estimates' degrees of freedom. Spikes in the time series were removed and replaced with linearly interpolated values.

A suite of programs entitled 'DIrectional WAve SPectra Toolbox for Matlab' (DIWASP), A Directional Spectral Wave Estimation Tool (Johnson 2002), was utilized to estimate the wave spectra. Inputs to DIWASP included 1) time series of array data, 2) data type, 3) sensor coordinates, 4) array orientation, 5) water depth, 6) array depth, 7) sampling frequency and 8) spectral estimation method. The Iterative Maximum Likelihood Method (IMLM) of spectral estimation (Pawka 1983) was applied to compute the directional spectra. The pressure time series each contained 2^{14} samples, which were divided into 16 non-overlapping sections each 1024 samples in length. The resulting

directional spectra had 32 degrees of freedom and a frequency resolution of 0.005Hz. Directional resolution of the spectra was 1 degree.

Statistics were derived from the directional energy density spectra, $S(f,\theta)$, as follows. The k^{th} *moment* of the spectral density function, denoted m_k, is defined as

$$m_k = \iint f^k S(f,\theta) d\theta df \tag{5.1}$$

The k^{th} *angular moment* of the spectral density function, denoted dm_k, is defined as

$$dm_k = \iint \theta^k S(f,\theta) df d\theta \tag{5.2}$$

Peak wave direction, D_p, is defined as the direction with the highest energy integrated over all frequencies. Peak wave period, T_p, is defined as the peak of the 1D frequency spectrum.

Verification of Spectral Estimates

Two IMLM-derived wave statistics, peak wave direction and peak wave period, are correlated with those derived by WES using the Direct Fourier Transform method (Longuet-Higgins 1963) to determine the veracity of the estimated spectra. Both parameters exhibit strong correlation with the baseline WES data. IMLM peak direction (Figure 4.4, Plot A) exhibits less noise than the DFT method and has an r^2 of 0.88. The peak period (Figure 4.4, Plot B) computed by WES suffers from relatively low resolution (seen as large jumps in value) resulting in a lower r^2 value despite the good agreement of the values that is evident in Plot B. Pawka (1983) found that the IMLM method resolved the directional spreading of a spectrum significantly better than the DFT estimation method, which tends to 'smear' the energy over a broader range of directions than that of the real spectrum. Analyses of directional spreading and spectral width, presented in Chapter 5, are computed from these spectral estimates.

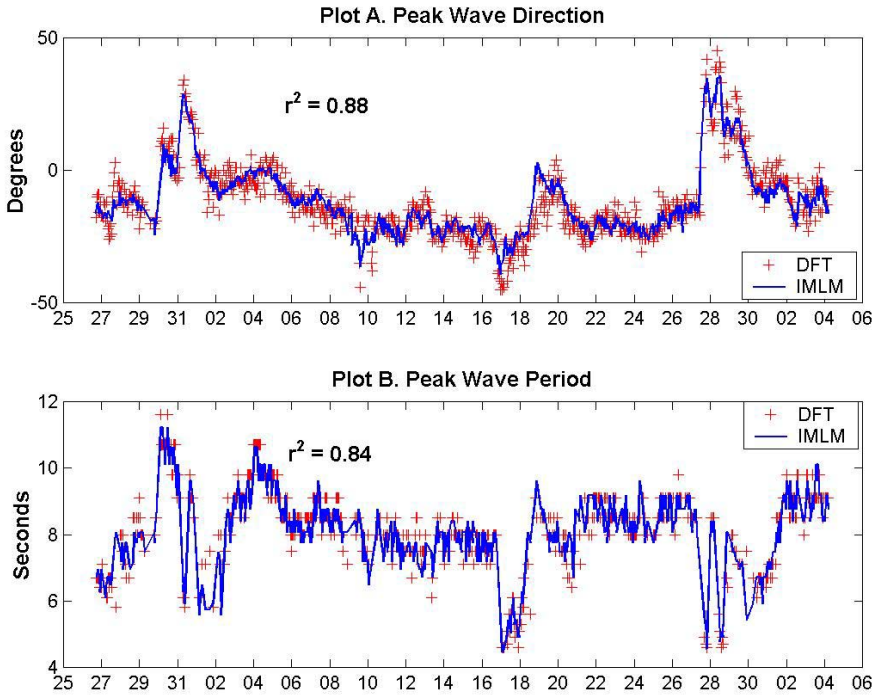

Figure 4.4: Correlation, r^2, of wave direction (Plot A) and wave period (Plot B) for the DFT and IMLM methods of spectral estimation.

CHAPTER 5
STATISTICAL ANALYSIS

The LURCS and ECFL LURCS scales presently in use were formulated by comparing rip current rescues and drownings in concert with the concurrent wind and sea state. Lushine (1991) and Lascody (1998) confirmed that rescue statistics provide a valid basis for the formulation of a forecasting technique. The present analysis was predicated on the assumption that the high numbers of beachgoers in Volusia County, and the high frequency of rip current rescues there, would allow a statistical analysis to be done to determine the conditions which pose the most risk to swimmers and to qualitatively assess the driving mechanisms of rip currents at the site.

One inherent limitation of using rip current rescue data as a proxy for rip current measurements is that the number of data points is typically very small when compared with traditional *in situ* instrumentation. An above-average day may have 20 rescues spread over the 6 hours: the data do not have fine-enough resolution to directly correlate rip intensity with phenomena that vary on time scales shorter than a day. This limitation means that it is not possible to cross-correlate time series of rip current (rescue) measurements with wave measurements and, thus, directly link them. As a result, wave parameters such as wave period, groupiness and narrow-bandedness, which are not independent of one another, cannot be singled out as the mechanism directly influencing rip current behavior. Rescue data is, however, well suited to a statistical analysis of the wave and wind conditions that were concurrent to rip current rescues. When taken as a whole, the long duration of rescue logs and large number of *total* rescues provides

valuable insight into the conditions that threaten beach-goers and constitutes a qualitative contribution to the understanding of rip current behavior.

Another important issue arose during analysis of the rescue data: the total number of swimmers at any given time is unknown. Statistics from the beach entrance ramps, where visitors are able to drive their vehicles onto the beach, could be used for this purpose, but are not available for 1996; thus, days with an unusually high or low beach population cannot be removed. For this reason, rip current rescues appear to mark the onset of dangerous rip current activity but become less reliable as the sea state becomes more energetic (and fewer persons entered the surf). Ideally, beach population data could normalize daily rip current rescue data resulting in more accurate assessments of rip current activity. This issue was particularly important to the verification of the predictive index, which will be discussed in Chapter 6.

In order to compensate for the lack of population data, the analysis was limited to only the times of highest beach attendance. Figure 3.1 illustrates the small number of rescues that occur October through February. An average of 16 persons per month were rescued from rip currents during those months versus over 100 persons per month for the remainder of 1996. Incident wave energy is generally significantly greater during the winter; thus, it is unlikely that the decline in rescues is due to weaker rip currents. Because of the colder water and air temperatures, few people enter the surf from October through February. In order in minimize the population effects of these low-attendance times only the period from March through September 1996 was considered for the following analysis. Similarly, the times of peak beach attendance are from 11am to 5pm daily (based on the rescue logs) and only those times were considered in this

investigation. This was particularly important for the wind direction analysis: during the summer, daytime wind is dominated by an onshore seabreeze and the inclusion of nighttime data would not statistically reflect the conditions encountered by swimmers. The restriction of the rescue statistics to only these dates and times reduced the number of rescues considered in this investigation from 686 to 612.

There were two sets of wave data utilized in this analysis, 1) long-term wave statistics computed by WES for the period from March through September 1996, and 2) short-term wave spectral statistics and groupiness computed from the original wave gage time series for the period from May 27th through July 6th 1996. These analyses are presented separately, owing to the significantly different length of time considered.

Long-Term Statistics.

Two wind parameters, three wave parameters, and tidal stage are statistically related with rip current rescues in this section. The double-bar histograms presented here represent the normalized frequency of rip current rescues for each wind and wave parameter (light colored bars) and the frequency for the entire record (dark colored bars) for the period. The entire record includes all hourly observations between 11am and 5pm during the months of interest. The number of observations were summed for each bin range and normalized by the total number of observations. The rip current rescue data are the wind and wave observations that were concurrent with each rip current rescue. For instance, if six persons were rescued between 2:30pm and 3:30pm on a given day, then the 3pm observations of each wind and wave parameter were recorded six times, one for *each* person. A total of 612 rescues were utilized for this analysis. The entire record (dark bars) are included as a baseline with which to compare the rescue statistics.

Of particular interest are the ranges of each parameter during which rip rescue frequency is significantly higher than that of entire record. These ranges represent a higher 'relative risk' of rip current activity that is threatening to the public and are the basis for improvements made to the rip current forecasting techniques (presented in Chapter 6). The sum of the squared difference (SSD) is presented on each plot. The combination of a high SSD and increased threat over a distinct range indicates that that parameter is well correlated with rip current rescues.

Wind Statistics

Previous studies by Lushine (1991) and Lascody (1998) utilized rip current-related rescues and drownings in concert with the concurrent wind speed, wind direction, wave height, wave period and tide data to formulate rip current forecasting techniques. Directional wave data are not commonly available along Florida's Atlantic coast and thus wave direction could not be included in those analyses. Both investigations found correlations between onshore-directed, high-velocity wind and increased rip current rescues and drownings. Archived shoreline wind data from 1996 were not available for Volusia County, so wind data from NDBC buoy 40009 was utilized for this analysis. This data likely does not detect the onshore-directed afternoon seabreeze, which occurs daily during warm months along the Atlantic coast of Florida; however, it represents the only reliable, archived wind data available for the study site.

In Figure 5.1, Plot A, wind speeds from 1 to 3.5 m/s had frequencies of rescue that varied only 5% over that range and account for 50% of the total rescues, indicating the rescue activity is relatively uniform over those wind speeds. The significance of mild wind conditions almost certainly is related to an increased number of beachgoers and swimmers on those mild days and not an increase in rip current activity due to low wind

speeds. A reduced number of rescues occurred after wind speed exceeded 8 m/s, which may be due to fewer people entering the surf. Wind direction, depicted in Figure 5.1, Plot B appears to have little relationship with the occurrence of rip related rescues, which is further evidenced by the very low SSD.

Wind speed and direction have not been positively correlated with rip current behavior elsewhere in the scientific literature; the effect of wind on the incident wave field is the likely source of the relationships noted by Lushine (1991) and Lascody (1998). Wind measurements represent a commonly available, though less effective, measure of the wave field in the absence of directional wave data. This investigation eliminates wind direction and speed from the forecasting technique based on the lack of statistical and scientific evidence linking wind direction and velocity with rip current strength. The present ECFL LURCS scale utilizes deep-water data for its predictions (NDBC buoys) and deep-water statistics provide a convenient reference point for future work. Because of this, data from the INT directional wave gage were shoaled and refracted to deep-water, assuming straight and parallel contours, using linear wave theory.

WES Wave Statistics

Figure 5.2 summarizes the relationships wave period, wave height, tide and wave direction have with rip current rescues. Wave periods from 7.5 to 9.0 seconds accounted for 62% of rip current rescues, and wave periods less than 6.5 seconds accounted for only 10% (Figure 5.2, Plot A). Wave period also has an SSD of 0.022; second highest of all of the predictive parameters investigated. These intermediate-period waves produce good surf and still allow beachgoers into the water resulting in increased frequency of rescues. Long period waves will be effected by the bottom at deeper depths and will break further

from shore, resulting in a larger wave set up. Long period waves may also have significance due to their potential 'groupiness' creating pulses in the rip currents

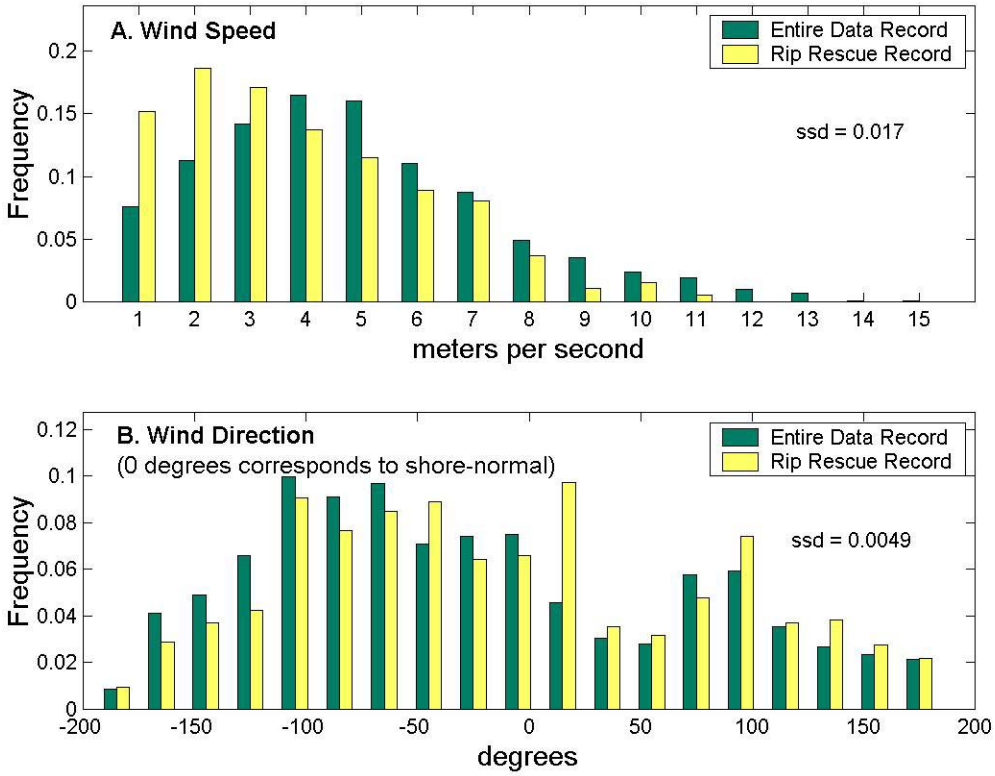

Figure 5.1: Normalized Frequency distributions for wind speed and wind direction, March through September 1996.

(Shepard and Inman 1950, Sonu 1972, and MacMahan 2003), which may catch bathers by surprise. Wave groupiness is discussed later in this investigation.

Figure 5.2, Plot B, shows 63% of all rescues occur with wave heights between 0.45 and 0.85 meters. Wave height also has the highest SSD among the variables, indicating a strong relationship exists between intermediate wave height and increased rescues. Rescue frequency falls off at higher wave heights even though rip currents themselves may well be stronger; this may be due to fewer people venturing into the surf during these rougher conditions or due to fundamental changes in nearshore circulation during

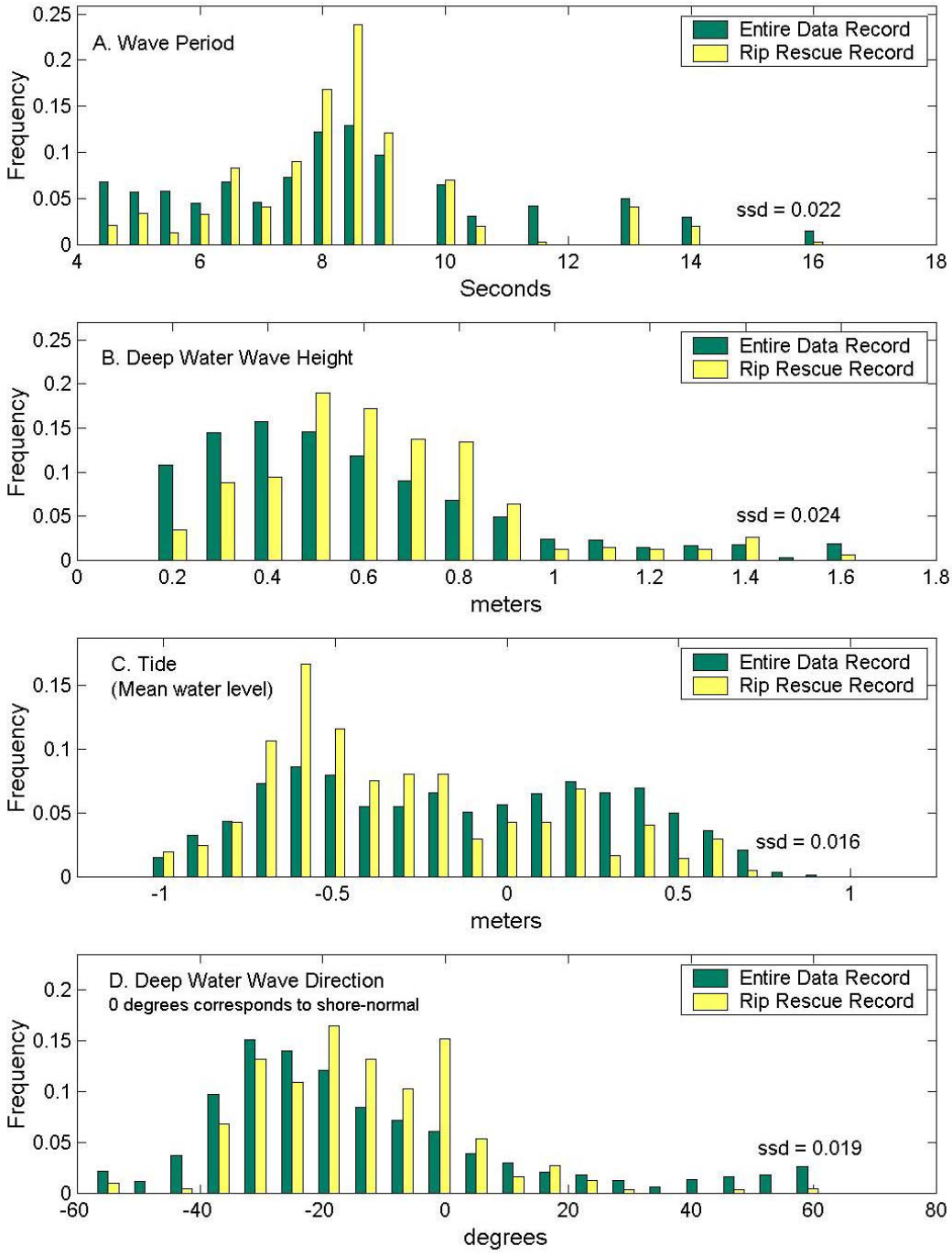

Figure 5.2: Frequency distribution of rip current rescues and the entire data record for tidal stage and wave parameters, March through September 1996.

higher energy. Wave heights lower than 0.45 meter still produced almost one quarter of the rip rescues, though, indicating rip currents of some strength are present even during mild conditions that occur often.

The rescue probabilities of wave height and wave period agree with the findings of Lushine (1991) and Lascody (1998): higher waves and longer period waves result in significantly higher rip current threat up to a certain threshold. Extremely high wave heights are not responsible for proportionally higher rescue numbers, possibly owing to either to reduced population or changes in nearshore circulation during high-energy events.

Mean water level (Figure 5.2, Plot C) appears to be an important parameter in the occurence of rip currents. The range from –0.75 to –0.45 accounts for 62% of the rescues while the tide occupies that range only 42% of the time. As the mean water level drops, waves break further from shore and the set up is increased between the shore and bar. At the same time the depth of water over the bar is reduced and the rip channels become more efficient pathways for water to leave the surf zone. The position of the breaking waves directly over the bar may also influence the strength of the rip currents (Sonu 1972). Sonu 1972, Brander 1999, Brander and Short 2001, and Dronen et al. 2002 all observed modulations of rip current strength associated with mean water level, with the rip current velocities reaching a maximum at low-tide. It is interesting that as the mean water level drops below –0.7m, the frequency of rescues becomes more like the overall frequency. It has been observed that the bar is exposed in some areas at very low mean water levels, which would stop cell circulation altogether.

Wave direction is depicted in Figure 5.2, Plot D; zero degrees corresponds with shore-normal waves and positive directions are counter-clockwise from shore-normal. Wave direction has a strong correlation with rip current rescue activity. Wave directions

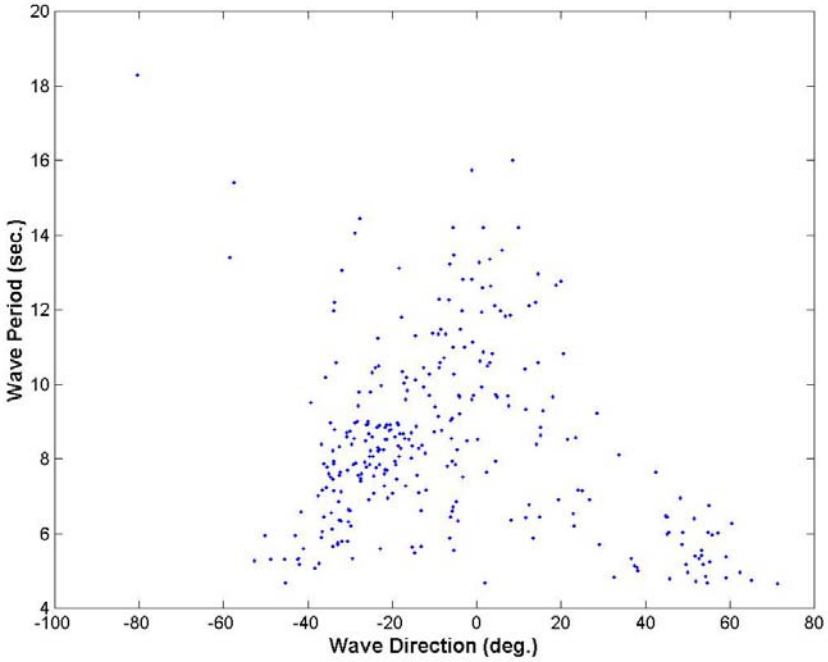

Figure 5.3: Daily average wave direction and wave period, January through December 1996. Greater directional variability at low wave periods indicates that the variables are not independent.

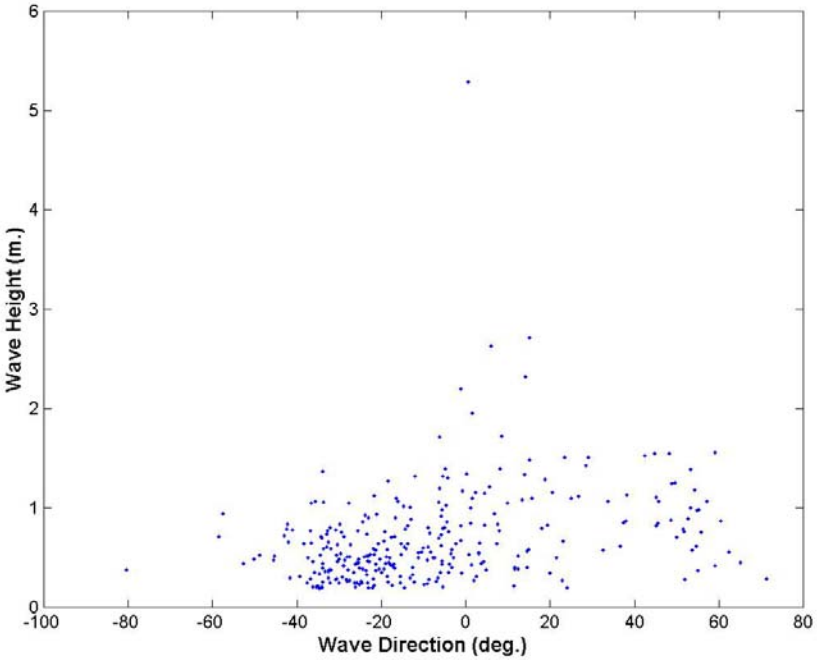

Figure 5.4: Daily wave direction and wave height, January through December 1996. Lower wave heights are strongly related with wave directions from –40 to –20 degrees indicating that they are not independent of one another.

between 4 and –20 degrees account for 56% of rescues while waves occur in that range just 31% of the time. Only 6% of rescues occur when the direction is less than –38 or greater than 16 degrees, while waves occur in those ranges 22% of the time suggesting that rips seldom formed or were weak under large oblique wave angles. The SSD of wave direction is 0.019. The rescue frequency is skewed toward negative angles, which is evidence that the wave direction is likely not independent of the other variables. In Figure 5.3 the wider distribution of wave directions at lower wave periods and the grouping of days at –25 degrees and 8 seconds shows that wave direction and wave period are not independent. Similarly, Figure 5.4 shows a grouping of days with wave directions of approximately –30 degrees and wave heights of less than 0.5 m. Positive wave angles, in general, are accompanied by higher wave heights. Overall, negative wave angles are associated with non-storm conditions consisting of moderate wave periods and low wave energy, while the positive wave angles are associated with higher waves and very short wave periods. The interdependence of these variables precludes the use of multivariate regression, which requires that all of the input variables be independent of one another.

Anecdotal evidence from the beach patrol staff suggested that rip current-related rescues may occur more frequently during outgoing tide; however, this observation is contradicted by the data. Figure 5.3 illustrates that the probability of rescue is not significantly higher during ebb flow (negative values); rip current rescues are divided nearly equally between ebb and flood flows. Variations of rip current strength are evidently dependent on the mean water level rather than the gradient of the mean water level.

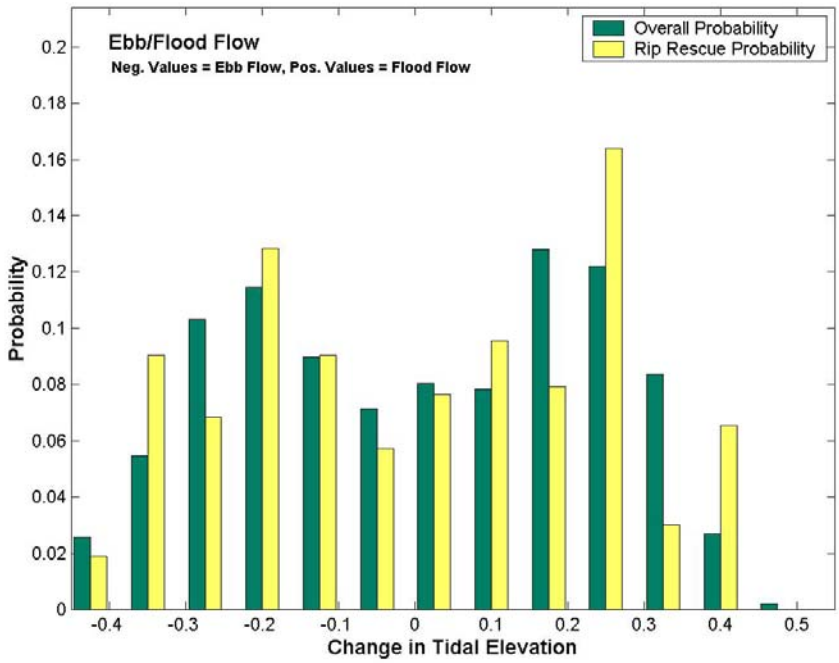

Figure 5.3: Probability of rip current rescue during ebb tide (negative values), flood tide (positive values) and slack tide (zero values). No correlation was apparent between the frequency of rescues and either ebb or flood tide.

Short-Term Statistics

For these analyses, WES provided some of the original wave gage data from the Ponce de Leon CIRP experiment to the University of Florida. Time series data from the wave gages are only available for the period from May 27th to July 6th 1996, so a long-term analysis of the wave groupiness and wave spectra is not possible. Three additional relationships are explored between the incident wave field and rip current rescues, 1) wave groupiness, 2) narrow-bandedness, and 3) directional spreading. Because of the uncertainties inherent in shoaling and refracting a wave spectrum to deep water (as was done to the long-term wave statistics), the directional spreading and narrow-bandedness are reported at the INT gage. Wave groupiness at both the INT and EBB gages are also related to rip current rescues.

Three distinct rip current rescue events occurred during this period, 1) on June 5th 31 people were rescued, 2) on June 19th 30 people were rescued, and 3) from June 28th to July 1st 85 people were pulled from rips. In fact, 48% of the rip current rescues (295 of the 612 included in the long-term analysis) took place during this five-week period. Thus, although the duration of this record is short, the statistics still represent a significant portion of the year's rescues.

Sonu (1972) attributed pulsations of rip currents to wave energy in the infragravity band (0.004—0.4 Hz). MacMahan et al. (2003) showed that significant pulsations in the velocity record of rip currents measured on a high-energy beach were forced by long-wave interactions and that the source of those long waves are short-wave groups. Groups of higher waves will lower the mean water level resulting in a long wave that has a period on the order of the group period (25 to 250 seconds). The infragravity motions summarized above were found to induce rip current modulations that were superimposed on the mean velocities of the rip currents. The best location for an instrument to directly detect infragravity energy is in the surf-zone, where short waves have broken and the infragravity energy is proportionally much more significant (MacMahan 2003). In the absence of these data, deep-water measurements are best suited to detecting the wave groups as opposed to the infragravity energy. To detect the possible importance of infragravity energy (and thus pulsations) as it relates to rip current hazard, wave groupiness as parameterized by List (1991) and narrow-bandedness, described by Longuet-Higgins (1975), are statistically correlated with rip current rescues.

The correlation between shore-normal wave incidence and higher rip current rescue frequency (Figure 5.2, Plot D) indicates that rip current strength is modulated by the

wave direction. Sonu (1972) observed that shore-normal wave incidence produced rip currents while oblique wave incidence induced longshore currents. Based on this assumption, and all other factors being equal, a shore-normal incident wave spectrum with narrow directional spreading would have more shore-directed radiation stress than a spectrum with wide directional spreading. Under these circumstances, less energy would be transmitted in the longshore direction and a greater proportion of the total energy would be directed at the shore creating both an increase in mass transport over the bar and greater setup at the shore. To test this hypothesis, directional spreading is statistically related to the rip current rescue data.

Groupiness

A groupiness parameter was conceived by List (1991) to parameterize the relative strength of wave groups. Pressure time series with $n = 2^{14}$ samples (corresponding to 55 minutes at 5 Hz), were converted to sea-surface elevation using the linear Fourier transform method. An envelope function, $A(t)$, is computed from the sea surface time series as follows. First, the sea surface time series, $\eta(t)$, is high-pass filtered with a cutoff frequency of 0.04 Hz to remove infragravity energy from the signal. Next, the absolute value of the resulting 'short wave' signal is found to introduce envelope-related variance to the series. Taking the absolute value effectively doubles the frequency of the signal. Next, $|\ \eta(t)\ |$ is lowpass filtered with a cutoff frequency of 0.08 Hz; the resulting signal is essentially a running mean. Finally, the lowpass filtered $|\ \eta(t)\ |$ is multiplied by $\pi/2$, which produces the envelope function $A(t)$.

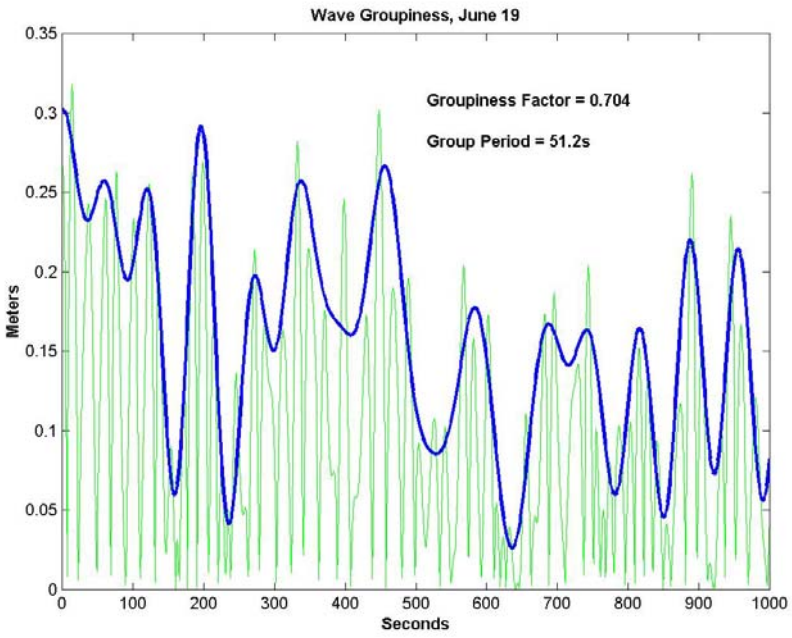

Figure 5.4: Absolute value of the high-pass filtered short-wave time series (light line) and the wave envelope (bold line) on June 19, 1996.

Figure 5.4 depicts 1000s of the absolute value of the lowpass filtered time series and the corresponding wave envelope. A groupiness factor, *GF*, was parameterized by List as a dimensionless function of the standard deviation, σ_A, and mean, μ_A, of the wave envelope as follows

$$GF = \frac{\sqrt{2}\sigma_A}{\mu_A}$$

The GF is a normalized standard deviation or coefficient of variation, which ranges from 0 for monochromatic waves to 1 for two beating sinusoids.

Figure 5.5 depicts the groupiness at the EBB gage location (Plot A) and the INT location (Plot B). The ebb gage exhibits correlation over a distinct range of values from 0.65 to 0.70, whereas, the INT gage has a less distinct range of higher rescue probability. The EBB gage was located in 7m water depth, half that of the INT gage. This might have allowed for a stronger wave-group signal due to shoaling. Although both locations

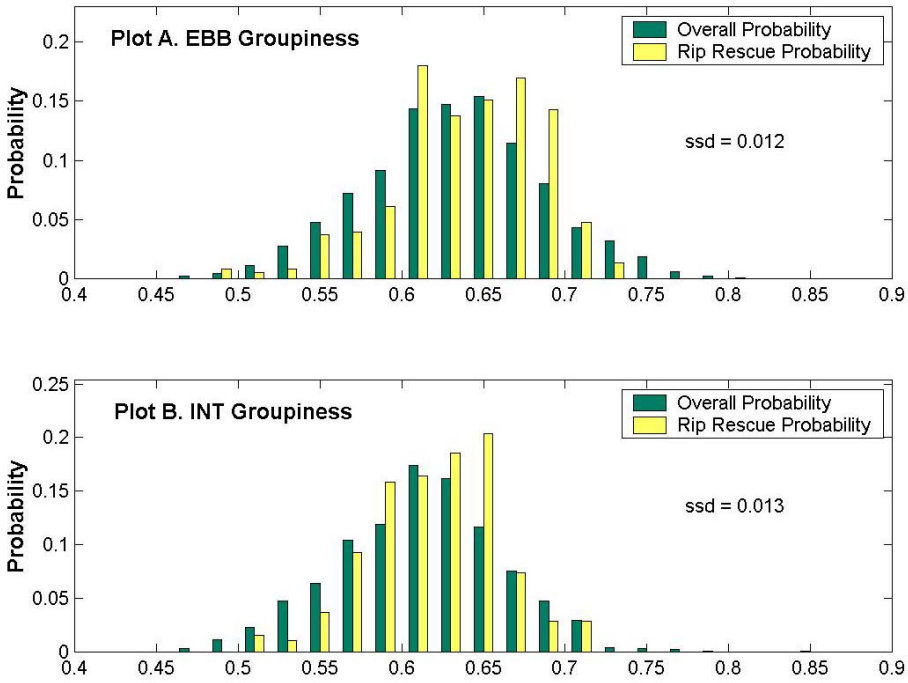

Figure 5.5: Wave groupiness at the EBB wave gage (A) and at the INT wave gage (B).

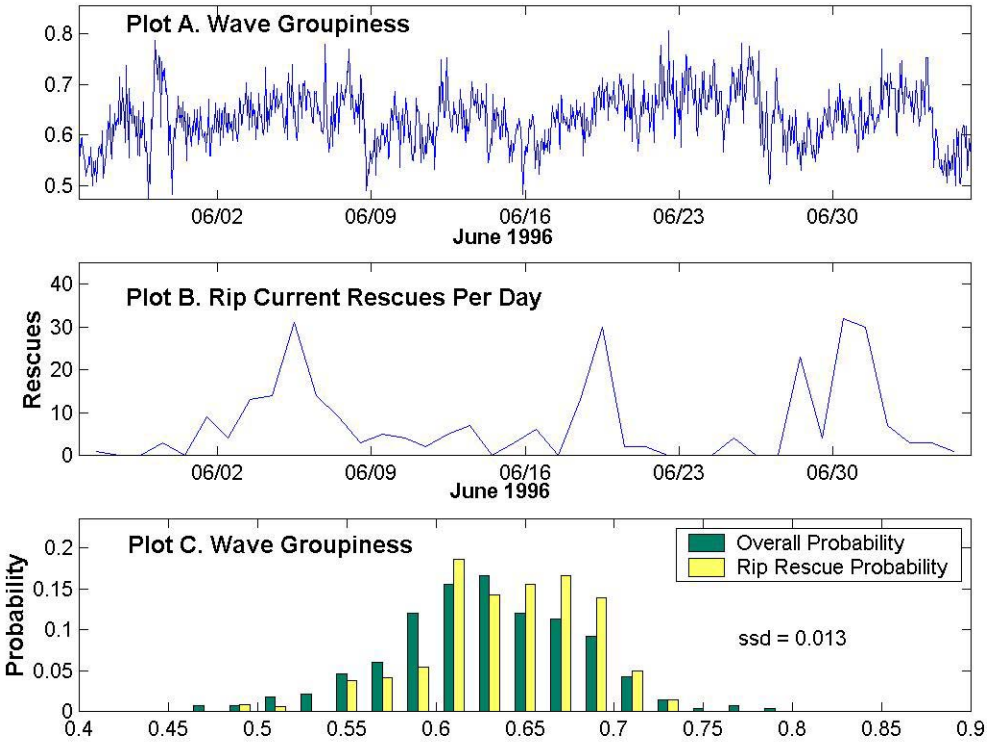

Figure 5.6: Time series of wave groupiness at the EBB gage (A), time series of daily rip current rescues (B) and probability of wave groupiness values (C) for the period from May 27th to July 6th, 1996.

indicated higher rescue frequencies occur at higher groupiness values, the EBB location was determined to be a better measure of the wave groupiness at the shore, thus the following analysis concentrates on the EBB gage data.

Rip current rescues occur more frequently (Figure 5.6, Plot C) when the groupiness is above 0.6 and significantly less when the groupiness drops below that value. Interestingly, when the groupiness is very high, there is little difference between the rescue frequency and the overall frequency. The large rescue events all occurred while the groupiness was trending higher (Figure 5.6, Plot A and B), but none of them are associated with the highest spikes in groupiness. The evidence appears to be inconclusive identifying groupiness as a predictor of rip current risk. This may indicate that pulsations do not pose a significant risk to swimmers in Volusia County; however, given the less than ideal position of the wave gage for a true measurement of infragravity energy, more research will need to be done to confirm this.

Spectral Width

The spectral width parameter ν, which is a dimensionless measure of narrow-bandedness (Longuet-Higgins 1975), is formulated as follows

$$\nu = \sqrt{\frac{m_0 m_2}{m_1^2} - 1} \tag{5.6}$$

The value of ν varies from 0 for narrow-banded to 1 for broad-banded processes. Rip current frequency (Figure 5.7, Plot C) is slightly higher than the baseline overall probability for spectral width values from 0.18 to 0.25; however, values from 0.27 to 0.29 still represent a significant portion of the total rescues. Rescues occur even at the relatively high value (for this data) of 0.33. The interaction between large rescue events (visible in Figure 5.7, B) and changes in the narrow-bandedness (Figure 5.7, A) indicate

that the large rescue events on 6/05 and 6/19 are characterized by slightly lower values; however, 6/17 had a value of 0.2, but there were no rescues recorded on that date. Rescue probabilities suggest that there may be a connection between narrow-banded wave spectra and increased rip current strength, but ultimately the correlations are too weak to be conclusive.

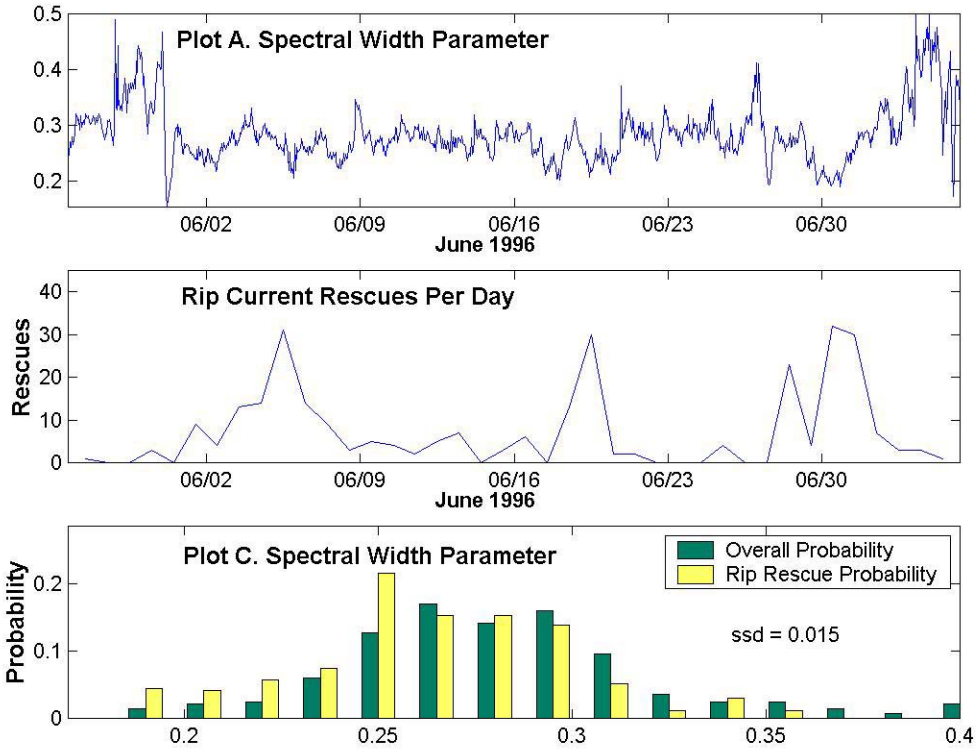

Figure 5.7. Time series of spectral width (A), time series of daily rip current rescues (B) and probability of spectral width (C) for the period from May 27th to July 6th, 1996.

Directional Spreading

Directional spreading, θ_s, is defined for this purpose as the rms angular deviation of the energy from the mean direction as follows

$$\theta_s = \sqrt{\frac{dm_2}{dm_0}} \tag{5.8}$$

where dm_2 is the second angular moment and dm_0 is the zeroth angular moment (Longuet-Higgins et al. 1963). The numerical value of θ_S is smaller for a spectrum with narrow directional spreading and larger for greater spreading.

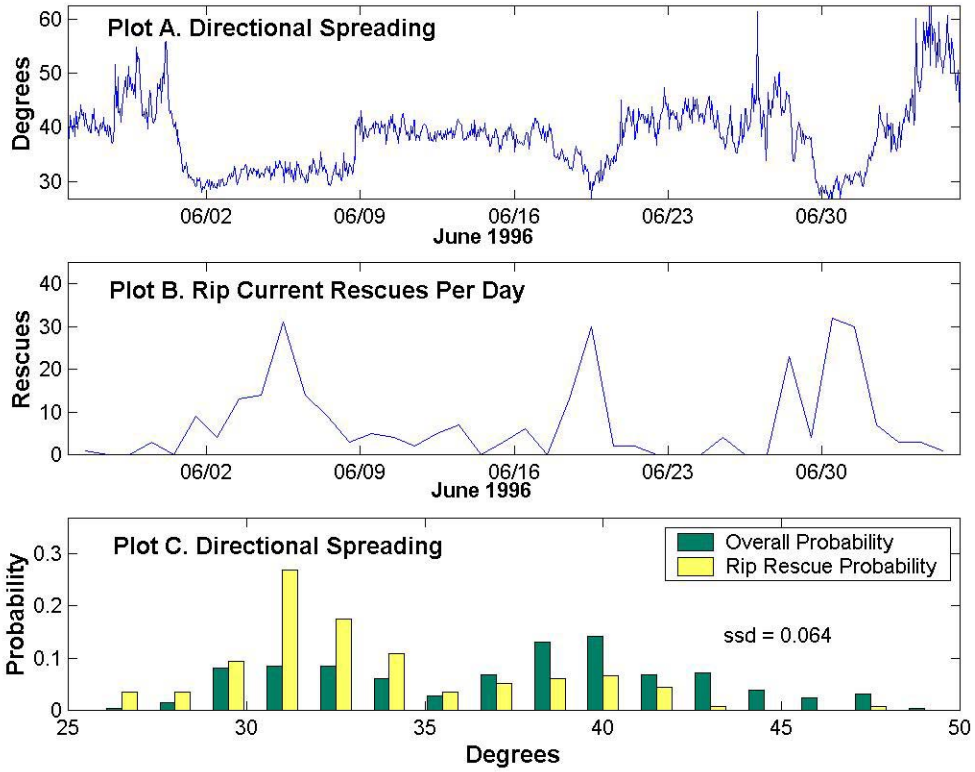

Figure 5.8: Time series of directional spreading (A), time series of daily rip current-related rescues (B) and probability of directional spreading (C) on Daytona Beach, FL for the period from May 27th to July 6th, 1996.

Of the short-term statistics investigated, directional spreading exhibited the most compelling connection with rip current rescue frequency. Directional spreading less than 35 degrees accounted for 75% of rescues while waves occurred in that range just 37% of the time suggesting rip current strength is inversely proportional to directional spreading (Figure 5.8, Plot C). Rip current rescues (Figure 5.8, Plot B) increased dramatically on 6/19, 6/30, 7/1 corresponding to narrow directional spreading; however, the high number of rescues on 6/05 take place during a period when directional spreading is not changing

significantly, which suggests that perhaps a combination of factors may have contributed to that event. Based on the statistical data, directional spreading significantly influences rip current strength: narrow directional spreading coincides with four of the five rescue events in excess of 20 persons that occur during the short-term analysis.

Discussion

Previous studies and the statistical analysis presented here indicate that rip current behavior is dependent on a combination of factors. The inability of rip current rescues to provide continuous rip current information and the interdependence of the variables prevents a multivariate regression of the data; however, the long duration of the data provides the opportunity to qualitatively assess scenarios that lead to large rescue events. In order to better understand the interaction of the wave parameters outlined in the above analysis it is helpful to view all of the variables at once, along with the rescue data. Of particular interest are the very-high risk days that have high rescue totals. The ability to detect these conditions is particularly important for rescue personnel. High rescue days also provide dense enough data to investigate tidal influences on rip current behavior in more detail.

Figure 5.9 illustrates the time series of peak period (A), wave direction (B), wave height (C), directional spreading (D) and daily rescues period (E); directional spreading is available only for the short-term period. The period presented in Figure 5.9 encompasses all days in 1996 with rip current rescues in excess of 20 persons. The wave event on 6/18 was tropical storm Arthur, which produced 75 km/hr winds and produced seas of 1.5 meters at the INT wave gage. On 7/11 wave heights peaked at nearly 4 meters from Hurricane Bertha, which packed 185 km/hr winds. Finally, Hurricane Eduard passed on 9/1, with wind speeds of over 185 km/hr for eight days straight, creating peak wave

heights of nearly 3 meters and causing failure of both the USACE wave gages and the NDBC wave buoy. As a result of the gage failures, no wave data is available for the peak in rescues that occurred on 9/1 and that day is left out of the following analysis.

Rescue peaks on 6/5, 6/19, 6/30, 7/1 and 7/13 (Figure 5.9, D) coincide with wave conditions that can be characterized by declining energy, relatively shore-normal waves and, where data are available, narrow directional spreading. Wave angles were near shore-normal and the sea more energetic in the days preceding each of these events suggesting rips may have been stronger; however, previous analysis has indicated that rip current rescues are less reliable during very high-energy events. Lascody (1998) noted that large numbers of rip current rescues occur with the following sequence of events, 1) strong onshore winds (and presumably high wave energy) cause people to stay out of the water, 2) as winds subside and the sea becomes less choppy, people venture back into the surf; however, the wave energy is still sufficient to cause dangerous rip currents and high numbers of rescues occur. The wind analysis from the present data (Figure 5.2) indicates that there is no positive correlation between rescues and concurrent wind measurements. This result suggests that wind direction, speed and duration affect the incident wave field, which in turn dictates the strength of rip currents even after wind velocity has dropped.

The statistical analysis of tide, presented in Figure 5.3.C, indicates that mean water elevations from –0.75 to –0.25 meters strengthen rip currents. Figure 5.10 depicts the distribution of rescues over the tidal cycle for each of the eight high-risk days. Except for 6/05, the peak number of rescues for each day occurred while the tide was between -0.25 and –0.6 meters and few rescues were recorded when the tide was +0.5 meters or higher, which agrees with the trends in the statistical analysis. On six of the eight days,

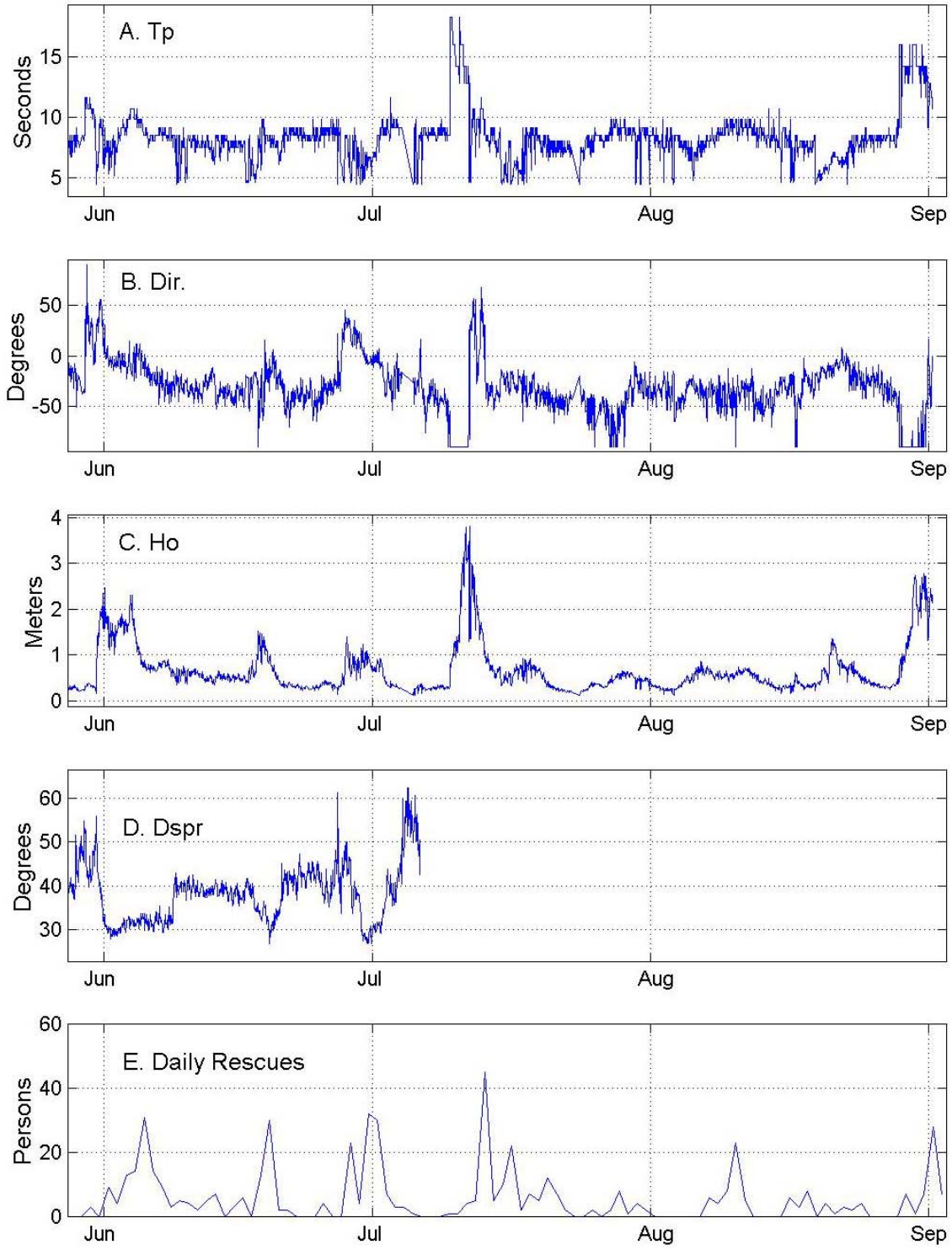

Figure 5.9: Time series of A) peak period, B) wave direction, C) wave height, D) directional spreading, and E) daily rescue totals for the period from May 30th to September 2nd 1996.

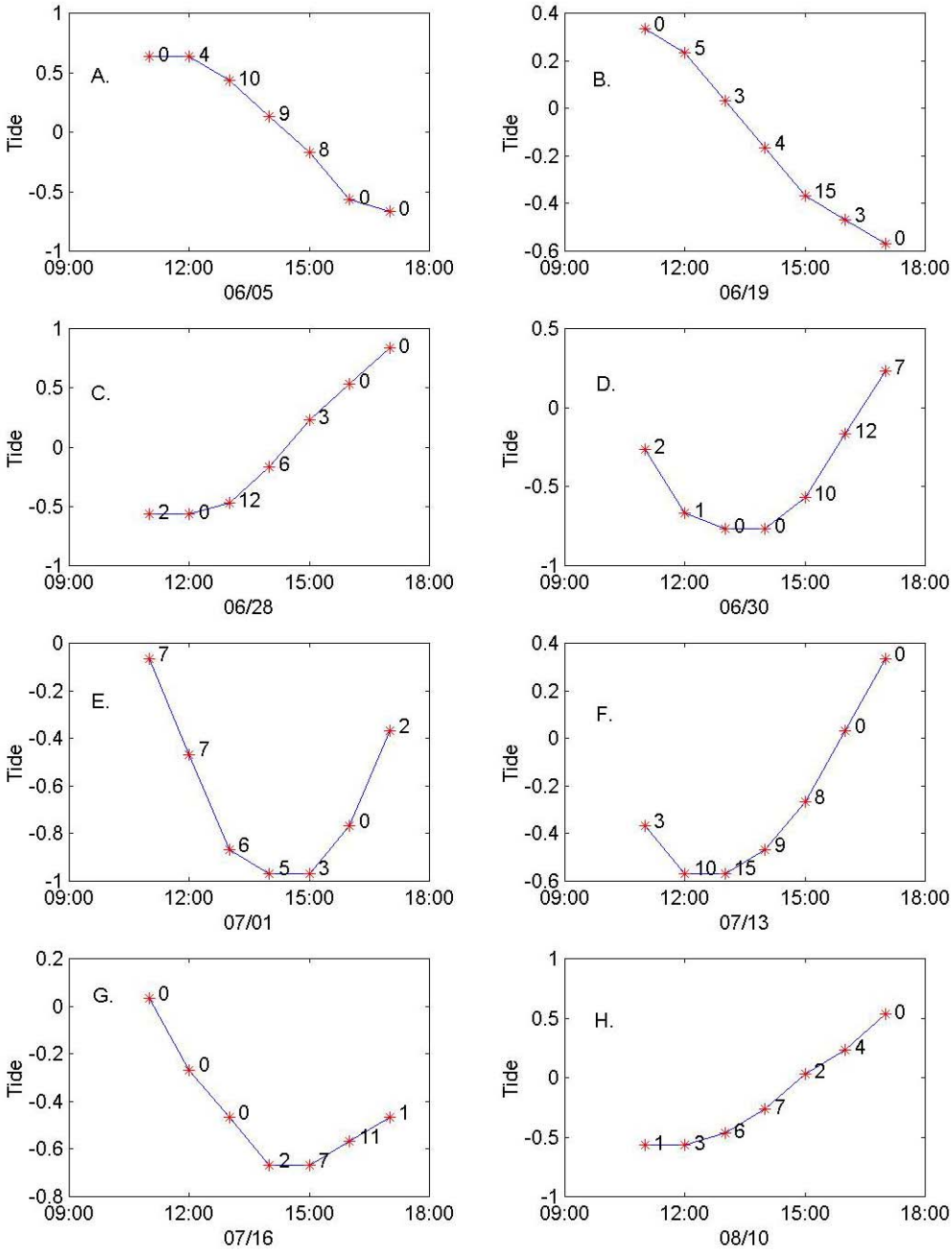

Figure 5.10: Tidal elevation and rip current rescue totals for eight days in 1996 with rescues in excess of 20 persons. Horizontal axes are local time; hourly rescue totals are displayed; the date is below each plot.

low tide occurred between 12:00 and 15:00 when, presumably, the beach would be the most crowded. The combination of wave conditions mentioned above and low tide occurring during the afternoon peak in population all appear to contribute to high rescue totals.

Declining-energy events appear to cause high risk conditions for several reasons, 1) wave heights are in the 0.5 to 1.0 m range characteristic of the highest rescue probabilities (see Figure 5.9, Plot B), 2) wave angles are relatively shore-normal after the energy subsides, 3) directional spreading is narrow after the storms (in fact, local minimums of directional spreading on 6/19 and 6/30 correspond with peaks in rip current rescues), and 4) it can be inferred that beach population increases significantly after the high winds and rough seas of storm events have subsided somewhat. If these conditions are coincident with low tide in the early afternoon, the conditions appear to be the most dangerous for swimmers. Surf-zone morphology may also play a part in the high relative risk of declining-energy conditions. In general, rip channels may deepen and become narrower after large wave events. The lower resistance of these hydrodynamically efficient channels may strengthen the rip currents until the channels widen and become shallower again. The lack of bathymetric data prevents an analysis of the bar and channel morphology at this time.

Improvements to the ECFL LURCS rip current forecasting techniques, presented in the Chapter 6, are based on the statistical analysis presented here. The factors that lead to high rip current risk are summarized as follows:

- Wave heights from 0.5 to 1.0 meters
- Wave periods from 7 to 9 seconds
- Wave directions from –20 to 4 degrees
- Mean water levels (tide) from –0.75 to –0.25 meters
- Directional spreading from 30 to 35 degrees

CHAPTER 6
MODIFICATION OF THE FORECASTING TECHNIQUE

Beach Patrol staff have noted that the greatest benefit to public safety would be the ability to more accurately predict, and thus prepare for, the relative strength of rip currents. At least one rip current rescue occurred on 66% of the days during the summer months of 1996, which implies that rip currents are nearly always present. This assumption was reinforced by the beach patrol staff, who are accustomed to making multiple rip current rescues on a daily basis. The present ECFL LURCS technique predicts the presence of rip currents and has been sufficient for issuing warnings to the public; however, it has not been utilized by the beach patrol due to its limited ability to discern between average rip current strength and high rip current strength.

The intentions of this investigation were to determine whether tidal stage and the incident wave climate had any correlation with rip current rescue activity in Volusia County and, more importantly, to use that information to improve the forecasting of rip current threat. The existing ECFL LURCS scale (see Figure A.1 in Appendix A) was used as a foundation for the new forecasting scale so that a legitimate assessment could be made of the new parameters' (wave direction, tide and directional spreading) viability as predictors.

The predictive index values for the new parameters were established based on the probabilities depicted in Figures 5.2, C (tide), 5.2, D (wave direction) and 5.8, C (directional spreading). Ranges of each parameter where the rescue probability was higher than the overall probability were assessed an index value of greater than zero:

larger differences of probability corresponded to larger index values in that parameter range. This subjective approach is taken due to the unreliable nature of the rescue data during high-energy conditions. Rescues decline when wave heights are above one meter and wave periods are greater than ten seconds—despite the fact that rip currents are most likely still strong. If the risk factors in the rip current scale were based strictly on the frequency of rescue, predicted rip current threat actually would decline during higher-energy conditions. The purpose of the scale is to predict the strength of the rip currents, not necessarily the conditions of maximum rescue. The rescue frequencies were used to establish the risk factors up to a point where the frequency appeared to be affected more by population than actual rip current strength. This approach was consistent with the formulation of the LURCS and ECFL LURCS indexes (Lascody 1998).A checklist for the modified ECFL LURCS index is presented in Figure A.2 in Appendix A. The wave period and wave height factors from the ECFL index were used in the modified index and were left unchanged.

Tidal Stage and Wave Direction

Data gathered from the NOAA, NDBC station 41009 data archive including wind speed, wind direction, wave height and wave period are used in the ECFL LURCS index for this study. Tidal stage and wave direction were added and wind speed and wind direction were removed as predictive parameters in the modified version of the scale. The modified scale utilizes wave data from the INT directional wave gage, including wave period, wave height, wave direction and tidal stage.

The National Weather Service gauged the performance of its existing scale by computing a Probability of Detection (POD) and a False Alarm Ratio (FAR). POD is the accuracy of the scale, and represents the percentage of rip current rescues that were

correctly detected by the rip current scale. POD is computed by summing every person rescued from a rip current during a day that was forecast to have rip currents and normalizing that value by the total number of persons rescued from rip currents on all of the days. The FAR is a measure of over-warning, which is the percentage of days that rip currents were predicted but no rescues occurred. The false alarm ratio is subject to error from a low population of swimmers due to weather or high-energy wave conditions: rips may be present but not marked by rescues. Thus, although improvements to the scale are marked by a reduction in false alarms, it cannot automatically be assumed that there were no dangerous rip currents present on days with no rescues.

A new measure was devised for this study called Alarm Ratio (AR). AR is the percentage of days that the scale predicted rip currents. The scales' utility is greatly diminished if it predicts rip currents too often so the modified ECFL LURCS' threshold of warning was established so that the alarm ratios of both scales were as close as possible. Improvements were then reflected in the POD, the FAR and the scales' ability to predict days with very high rescue totals.

An effort was made to assess the performance of the scales on an hourly basis so that the conditions concurrent with every rescue could be used in the rip current forecast; however, the rip current rescue record is too sparse on that short time scale and, for that reason, the performance of both forecasting techniques was erratic. As mentioned, previously, the number of rip current rescues that occur on a daily basis does not represent a continuous measure of rip current strength, so modulations of rip current strength that may occur on time scales shorter than a day cannot be detected reliably via rescue statistics. Both the LURCS and ECFL LURCS scales are computed by the NWS

on a daily basis, which is practical for issuing warnings to the public and for use by local authorities. This daily approach allows the accuracy of the prediction to be gauged by the total number of rescue *per day*, increasing the sample size. For these reasons, the rip current threat is calculated on a daily basis and compared with the daily rip current rescue totals to compute AR, POD and FAR.

The long-term wave direction and tide statistics represent over twice the number of samples as the short-term directional spreading statistics. For this reason, changes to the ECFL LURCS scale took place in two distinct stages, 1) analysis of tidal stage and wave direction as predictive parameters based on performance during the period from May through August, and 2) analysis of directional spreading as a predictive parameter for the period from May 27th through July 5th.

Addition of Long-Term Wave Direction and Tidal Stage

The long-term statistical analysis presented in Chapter 5 encompassed the period from March through September 1996. The longest possible period was chosen for that analysis to include as many of the rescues as possible, even though the rescue numbers for March, April and September were significantly lower than the middle summer months

A representative daily value for every parameter was computed from the hourly wind and wave measurements taken between 11am and 5pm. Mean values of wind speed, wave height and wave period were computed and median values of wind direction and wave direction were computed. Daily values from both the NOAA buoy and the Army Corps' directional wave gage were computed this way. Tidal stage presented a unique problem. The mean water level for each day, between 11am and 5pm was computed, but there was only a weak correlation with the daily rip rescue totals. The best correlation between rescues and tidal stage, on a daily basis, occurred when the minimum measured

tidal level for the day (6 hours, 11am to 5pm) was utilized. Figure 6.1 depicts the histograms for both minimum tide and mean tide. Both have the same SSD; however, minimum tide (Figure 6.1, A) retains the clear range of higher rip current probability between –0.6m and –0.8m that is evident in the hourly tide data (Figure 5.2, C). The mean tide (Figure 6.1, B), on the other hand, exhibits no clear trend of increased rip current rescue probability.

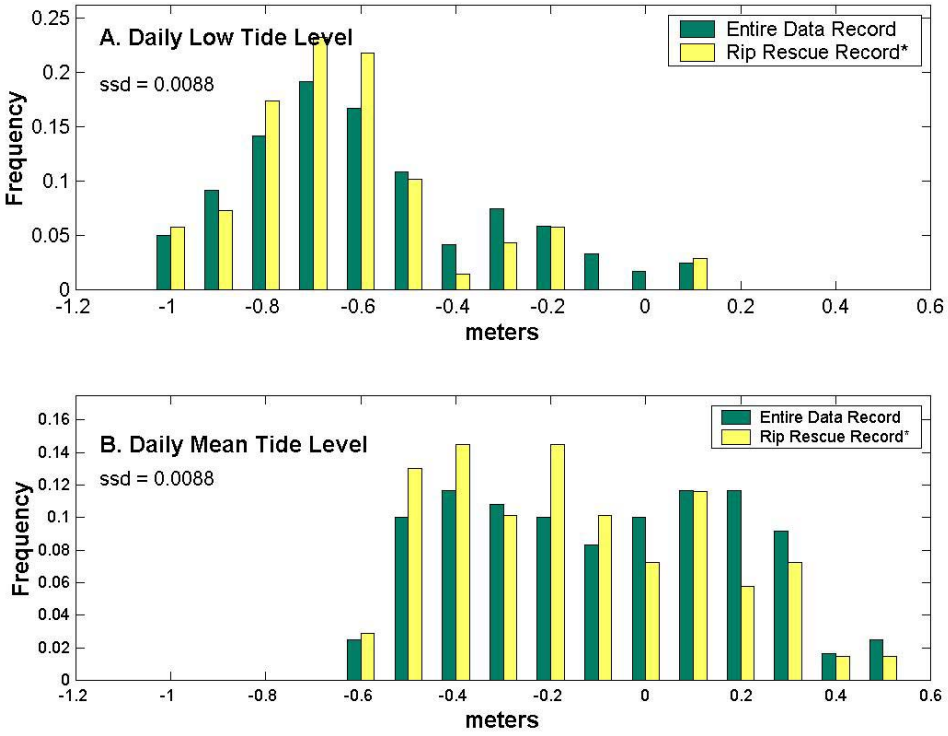

Figure 6.1: Rip current rescue probability for daily representative values of tide. Plot A is the lowest tide recorded between 11am and 5pm. Plot B is the mean tide during the same period.

Hourly rescue frequencies, shown in Figure 5.2 Plot C, suggest that a mean water level of around –0.6m is ideal for dangerous rip current activity and it is possible that

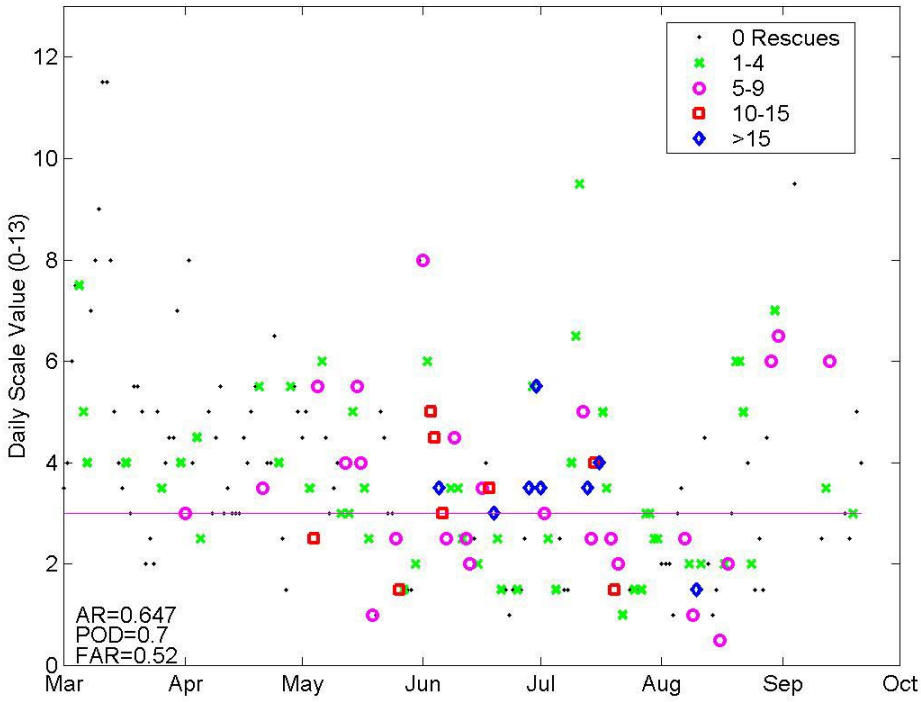

Figure 6.2: ECFL LURCS daily rip current index for the period from March through September 1996, including daily rip current rescue totals. Marker symbols represent the total number of persons rescued from rip currents on that day.

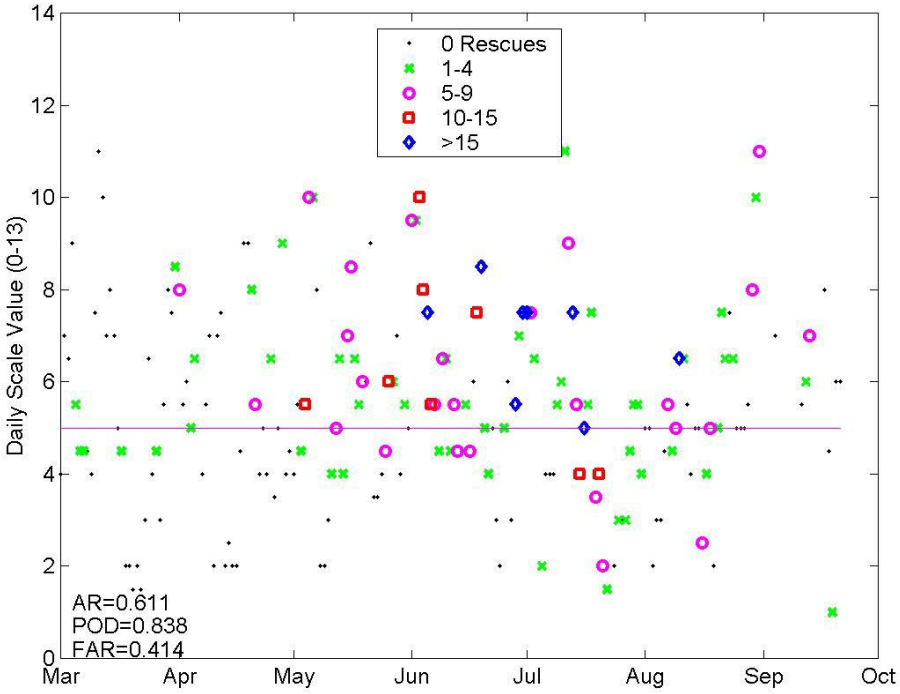

Figure 6.3: Modified LURCS daily rip current index for the period from March through September 1996, including daily rip current rescue totals. Marker symbols represent the total number of persons rescued from rip currents on that day.

detecting whether or not the tide reaches that range is a better indication of rip current activity than the value of the mean water level over the whole day. Figure 5.10 also indicates that the most hazardous conditions occur when low tide occurs between 11am and 5pm. The representative daily tide value used for input to the modified scale is the minimum tide occurring between 11am and 5pm.

Figure 6.2 depicts the rip current threat that the ECFL LURCS forecast for each day from March 1st to September 31st. Figure 6.3 depicts the rip current threat that the modified scale forecast for the same period. The vertical scale is the rip current risk as predicted by the indexes, which varies from 0 for no risk to 13 for maximum risk. The National Weather Service issues statements for a greater than normal threat of rip currents when the ECFL scale is 3.0 or above (2.5 or above on weekends or holidays), which is represented on the plot as a horizontal line. Additionally, the NWS issues very-high rip current threat when the scale is over 4.5 during the week or 4.0 on weekends or holidays. Different markers on the plot represent the number of rip current rescues that occurred each day. Modifications to the rip current scale include the addition of a modified tide factor, which increases rip current threat at mid-low tide and the addition of a wave direction factor, which increases as the wave angle approaches shore-normal. Both the wind velocity and wind direction factors were eliminated in the modified scale based on the statistical analysis presented in Chapter 5. Figure 6.3 depicts the performance of the modified scale. The threshold of warning for the modified scale was set at 5.0 (depicted as a horizontal line in Figure 6.3), so that the AR roughly matched that of the ECFL scale; forecasting improvements are reflected in the POD and FAR.

Both the POD and the FAR are improved by 20% in the modified scale during the period from March through September.

The high FAR in both of the scales may be the result of low population during March, April and September. The water and air temperatures during these months is lower and many of the days with high-risk predicted by the scales had no rescues whatsoever. Elimination of those months from the scales, depicted in Figure 6.3 and Figure 6.4, resulted in a nearly 40% drop in the FAR of both scales. In order to effectively assess the performance of the scales, April, March and September were removed from the rip current index testing.

Figure 6.4 depicts the ECFL LURCS scale for the period from May through August 1996. The alarm ratio shows that rip current warnings would have been issued on 51% of the days during the period. The POD indicates that the existing model successfully forecast 68% of the rip current-related rescues and the FAR indicates that 30% of the days forecast to have increased rip current threat actually had no rescues. The threshold of 4.5 for much greater threat would not have detected seven of the eight large rescue events that occurred. Figure 6.5 illustrates the modified scale's performance. Modifications to the index improved the POD 23%, while at the same time improving the FAR 14%.

There is a wide scatter of rip current scale values, in both the present scale (Figure 6.4) and the modified scale (Figure 6.5), for days with fewer than ten rescues. A lower number of rescues on a particular day could indicate rip currents were not as hazardous as days with higher rip rescues totals; however, it may only indicate that fewer people entered the surf when the rip currents were dangerous (due to rough surf conditions, foul

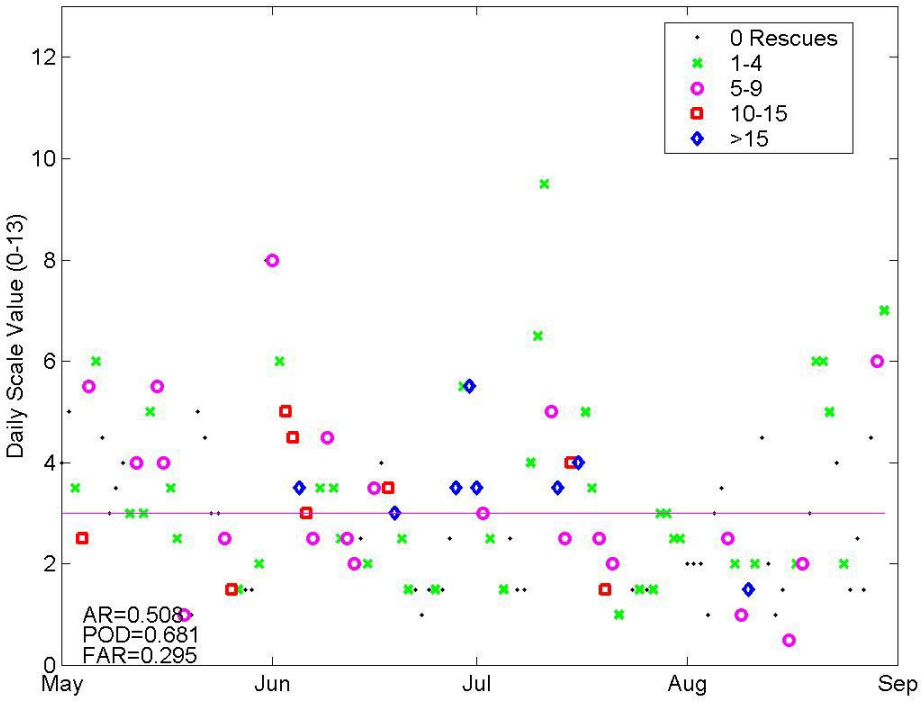

Figure 6.4: ECFL LURCS performance, May through August 1996. FAR drops by 40% when March, April and September were eliminated from the record.

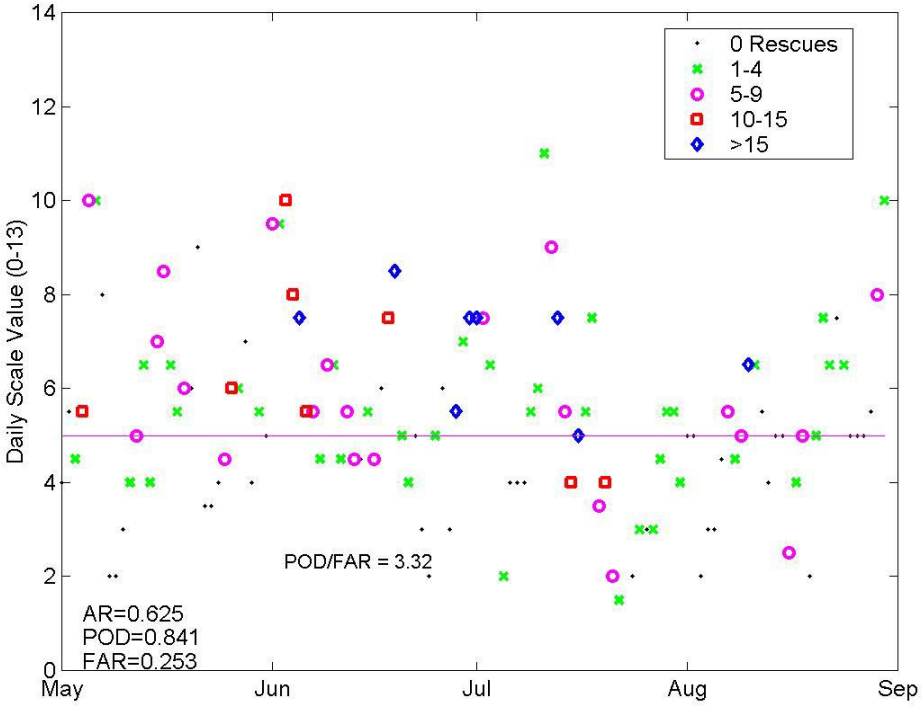

Figure 6.5: Modified scale, May through August 1996. FAR drops 41% when March, April and September are eliminated from the record.

weather, etc.). In other words, a low rescue total is not a conclusive measure of the intensity of rip current activity. High daily rip rescue totals, on the other hand, assure that hazardous rip currents most likely were active. In some cases, an unusually high rescue total may be related to a high number of beachgoers, but rip currents almost certainly must have been present. As a result, a forecasting technique's accuracy is its ability to detect large rescue events. The eight days in 1996 that had rip current rescues in excess of 15 persons (for which concurrent wave data are available) are summarized in Table 6.1. The ECFL LURCS scale forecast five out of the eight events; the modified scale forecast seven of the eight of these large rescue events, an improvement of 25%. Figure 6.5 also illustrates that modifications to the scale enabled it to better forecast days with rip related rescues in excess of nine persons: correctly predicting 14 of 16 events as opposed to 12 of 16 for the ECFL scale.

Table 6.1: Dates during the period from May through August 1996 with rip current related rescues in excess of 15 persons. Included are daily values for the deep water wave conditions, directional spreading at the INT gage and tidal stage along with the rip current forecast of both the ECFL LURCS and modified scales.

Date	Day of the Week	# Of Rip Current Rescues	Wave Ht. (m)	Wave Per. (s)	Wave Dir. (Deg.)	Dspr (Deg.)	Time of Low Tide	Level of Low Tide (m)	ECFL LURCS Alert	Mod. Scale Alert
6-5	Wed	31	0.56	8.8	-9	32	5pm	-0.7	Yes	Yes
6-19	Wed	30	0.62	7.9	-8	30	5pm	-0.6	No	Yes
6-28	Fri	23	0.83	6.9	+20	37	11am	-0.6	No	Yes
6-30	Sun	32	0.86	6.3	-5	29	1pm	-0.8	Yes	Yes
7-1	Mon	30	0.64	8.5	-3	31	2pm	-1.0	Yes	Yes
7-13	Sat	45	0.74	8.2	-23	n.a.	1pm	-0.6	Yes	Yes
7-16	Tue	22	0.74	5.7	-32	n.a.	3pm	-0.7	Yes	Yes
8-10	Sat	23	0.48	8.7	-18	n.a.	12pm	-0.6	No	Yes

In the previous section the threshold of warning was set so that the AR's were matched in the March through September plots and the improvements were reflected in the POD and FAR. A more systematic approach for setting the threshold is to optimize it

so that the ratio POD/FAR is maximized. Warnings issued at 5.0 result in a POD/FAR of 3.32; warnings at 5.5 result in a POD/FAR of 4.39; warnings at 6.0 result in a POD/FAR of 3.52. A threshold of warning at 5.5 for greater than normal rip current threat optimizes the modified scale's performance.

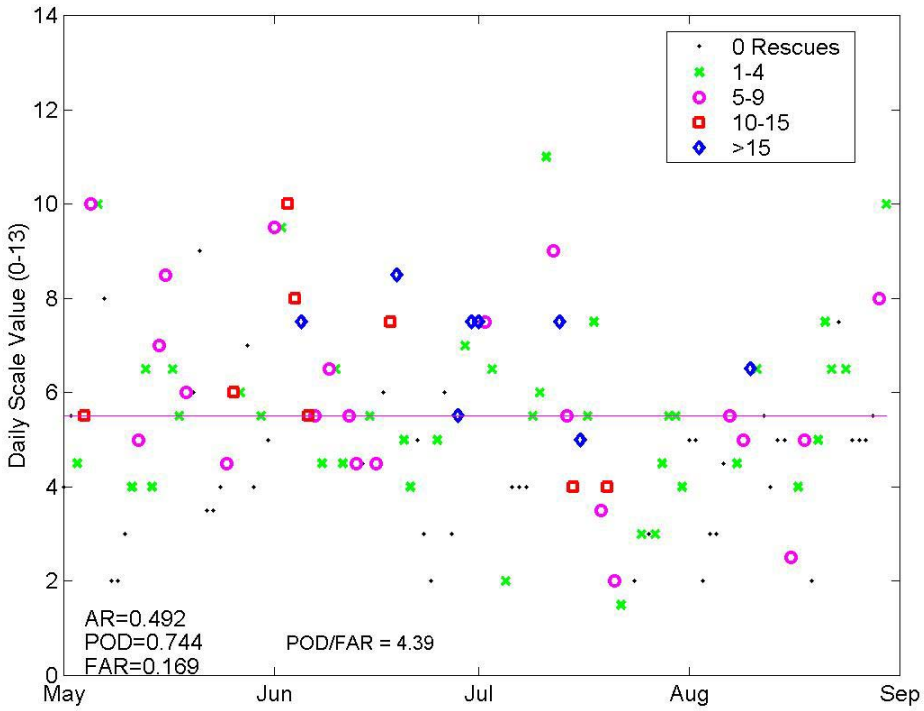

Figure 6.6: Modified scale performance with optimized threshold of warning. Maximum POD/FAR ratio occurs when the threshold is set at 5.5.

Addition of Directional Spreading

Correlation of three new wave parameters with rip current rescues based on 5 weeks of time series data were presented in Chapter 5. Those parameters included, 1) spectral width, 2) wave groupiness, and 3) directional spreading. Although all of the parameters exhibited some positive correlation with rip current rescue probability, directional spreading had the strongest correlation. For this reason it was decided that only directional spreading would be added to evaluate its validity as a predictor. Numerical index values for directional spreading were configured using the probabilities

represented in Figure 5.8, Plot C, which is similar to the methods employed by Lushine (1991) and Lascody (1998).

Table 6.2: Directional spreading factor included in the modified ECFL LURCS rip current forecasting technique. Numerical values for the factor were assessed based on statistical analysis of rip current rescues.

Directional Spreading	
Dspr, (θ°)	Factor
θ > 35	0
30 < θ <= 35	3
θ < 30	4
Dspr Factor =	

The following analysis was limited to the relatively short five-week period for which spectral wave data was available; however, significant improvements were evident when directional spreading was included as a predictive parameter. Figure 6.7 illustrates the performance of the modified scale without directional spreading as a predictive parameter; Figure 6.8 depicts the scale's performance after directional spreading was included. Both scales detected all of the high-risk events (days with 10 or more rip rescues); however, addition of the directional spreading factor (Table 6.2) more clearly differentiated High-risk events from low-risk events. A very-high threshold could be established at 9 that would only alert for the most dangerous days.

Alarm Ratio (AR), Probability Of Detection (POD) and False Alarm Ratio (FAR) are computed using the threshold as a cutoff point. The AR remains the same, thus, the threshold for warning remains the same. POD and FAR remain stationary with the inclusion of directional spreading, which is a reflection of the fact that it only greatly affects the very high risk days.

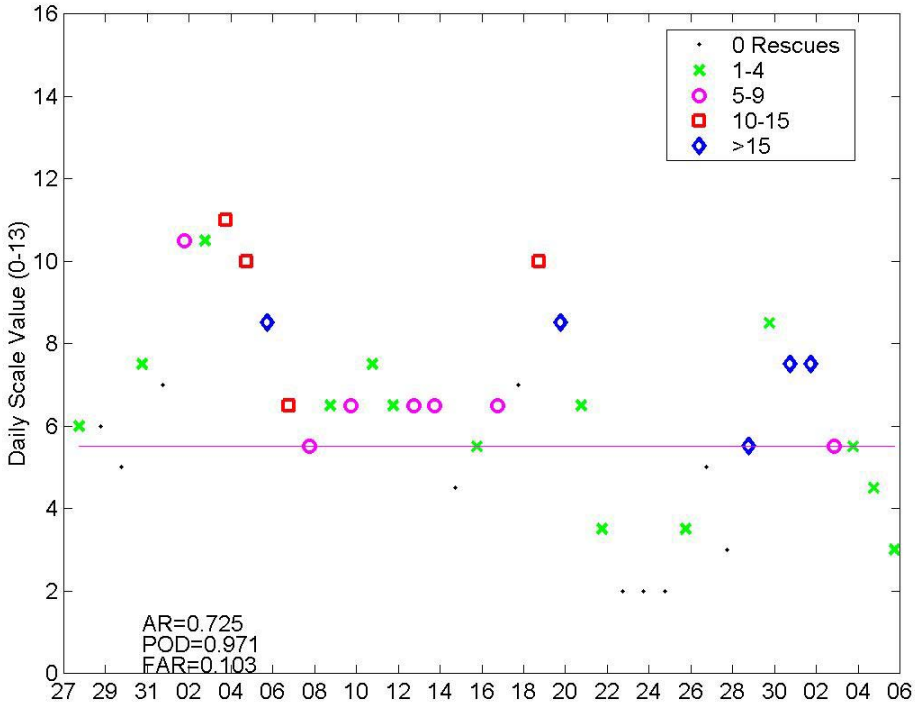

Figure 6.7: Modified LURCS daily rip current index, *without directional spreading as a predictive parameter*, for the period from May 27th through July 5th, 1996. Daily rip current rescue totals are indicated by marker symbols.

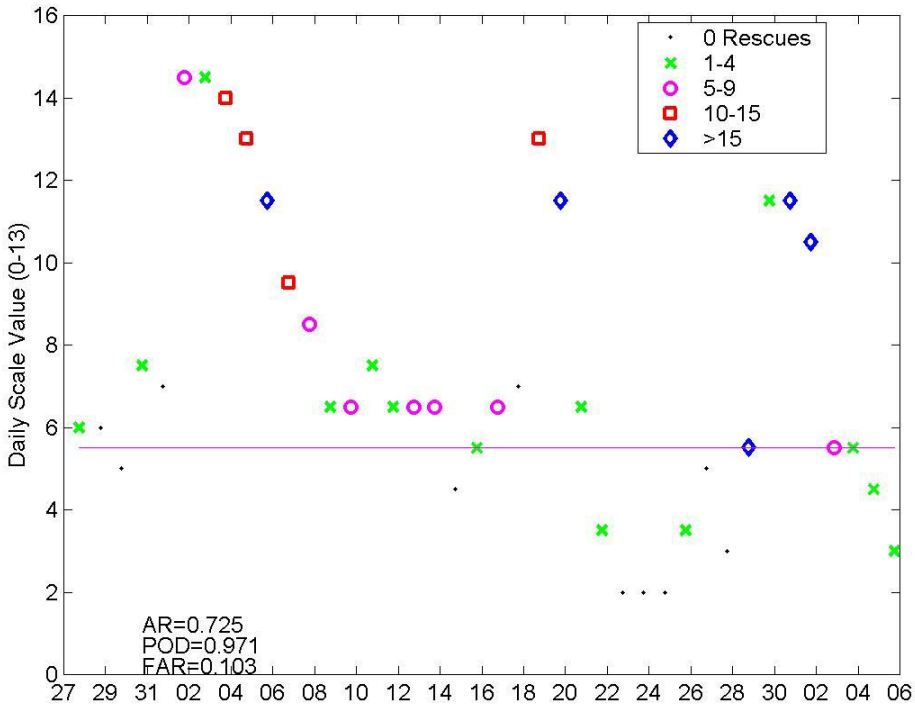

Figure 6.8: Modified LURCS daily rip current index, *including directional spreading as a predictive parameter*, for the period from May 27th through July 5th, 1996.

Wave direction and tide improved the scales accuracy and the inclusion of directional spreading increased its sensitivity to the declining energy events that characterized the peak rescue events. Narrow directional spreading is strongly correlated with a high frequency of rip current rescues as indicated by Figure 5.8, Plot C. In addition, the fact that directional spreading stays narrow after high-energy events have passed (and in some cases reaches its minimum after the event) improves the scales' accuracy at detecting very high-risk days.

A second threshold to detect high-risk events could be established based on further assessment of the modified scale when compared with rescue totals and rip current measurements by *in situ* instrumentation. A high-risk warning could alert beach patrol staff at the beginning of the day, so that staffing adjustments could be made or restrictions placed on swimming activity. The resulting index could be used as an effective assessment of the rip current risk for both issuing warnings to the public and for alerting beach patrol personnel. Despite the inherent difficulties of using rip current rescue logs to gauge the strength of rip currents, the improved performance of the modified scale proves that beach patrol rescue logs provide a readily available source of data on rip current behavior

Implications for Future Rip Current Investigations

The statistical analysis of rip current rescues has two distinct implications for future rip current study. One, it reaffirms the importance of mean water level and directional spectral wave data in the study of rip currents. Statistical analysis of the rescue data clearly indicates that the incident wave field and tidal stage modify rip current behavior significantly. Two, this research illustrates a framework for improving rip current prediction at other sites: analysis of rescue data is a valid approach for formulating rip

current forecasting techniques. The statistical approach utilized for this investigation can be applied in any location with significant numbers of rip current rescues and concurrent tide and directional wave data. There are a limited number directional wave gages and buoys that provide access to their data in real-time. These measurements are essential information for the prediction of rip currents risk.

CHAPTER 7
SUMMARY AND CONCLUSIONS

Lifeguard rescue logs from Daytona Beach, Florida were examined in an effort to correlate rip current-related rescues with concurrent wave and wind measurements on a barred shoreline with periodically spaced rip channels. The frequency of rip current rescues increased markedly during (1) shore-normal wave incidence, (2) mid-low tidal stages, (3) deep water wave heights of 0.5 to 1.0 meters, (4) wave periods from 8 to 10 seconds, and (5) wave spectrum directional spreading of less than 35 degrees. Very high risk days frequently take place following storm events when wave energy has declined to the point where people feel safe venturing back into the surf, but rip current intensity is still high, resulting in high numbers of rescues.

Rip current rescues appear to mark the onset of dangerous rip current activity but become less reliable as the sea state becomes more energetic. Daily beach attendance figures are not available for Volusia County, thus days with unfavorable sea state or weather conditions that keep beach attendance and swimming activity low are difficult to isolate and remove. Despite these weaknesses, rescue statistics offer one of the only long-term records of rip current activity that is widely available for study. Examination of the correlations between rescue frequency and wave conditions enables more accurate forecasting of rip current strength, which benefits public safety, and helps to shed light on the mechanisms that drive rip currents.

Three new predictive factors were developed to improve the ECFL LURCS scale: an improved tide factor, a wave direction factor and a directional spreading factor. The

inclusion of these new factors and the elimination of two wind scales were found to improve the accuracy of the ECFL LURCS scale in Volusia County. The modified scale more accurately forecast all rip current rescues and significantly improved detection of very-high risk conditions.

APPENDIX A
FORECASTING CHECKLISTS

1. WIND FACTORS	MOST FAVORABLE FOR RIP CURRENTS	MOST FAVORABLE FOR LONGSHORE CURRENTS
SPEED / DIRECTION	(40-110°)	(120-160°, 340-30°)
5 kt	0.5	0.0
5-10	1.0	**0.5**
10	1.5	1.0
10-15	2.0	1.5
15	3.0	2.0
15-20	4.0	3.0
20	5.0	4.0
20-25+	5.0	4.0
	WIND FACTOR	**0.5**

2. SWELL FACTORS		
a)	SWELL HEIGHT	SWELL HEIGHT FACTOR
	1 ft	0.5
	2	1.0
	3-4	**2.0**
	5-7	3.0
	8-10	4.0
b)	SWELL PERIOD	SWELL PERIOD FACTOR
	7-8 sec	0.5
	9-10	1.0
	11-12	**2.0**
	>12	3.0

c) **SWELL HEIGHT FACTOR + SWELL PERIOD FACTOR = SWELL FACTOR**	**4.0**

3. MISCELLANEOUS FACTORS	
If astronomical tides are higher than normal (i.e., near full moon), add 0.5	
If previous day **Wind Factor** or **Swell Factor** greater than or equal to 2.0/1.5, respectively, add 0.5	
MISCELLANEOUS FACTOR	**0.5**

4. **TODAY'S RIP CURRENT THREAT** is a summation of the 3 factors.	
LONGSHORE / RIP CURRENT THREAT	**5.0**

5. If RIP CURRENT THREAT is 3.0 - 4.0** (2.5 - 3.5 ** on weekends/major Holidays): issue statement for greater than normal threat of rip currents.

If RIP CURRENT THREAT is 4.5 - >5.0 ** (4.0 - >5.0 ** on weekends/major Holidays): **issue statement for much greater than normal threat of rip currents and/or heavy surf.**
** **(and it looks reasonable, e.g., an arctic outbreak, rainy day, hurricane, etc. is not occurring)**

Figure A.1: ECFL LURCS checklist (from Lascody 1998)

Modified ECFL LURCS Checklist

Example computations appear in ***bold***.

Wave Period	
Period, T (s)	Factor
T < 6	0
6 <= T < 9	***0.5***
9 <= T < 11	1
11 <= T <12	2
T >=12	3
Wave Period Factor =	***0.5***

Wave Direction	
Direction, θ (deg)	Factor
θ < -35 or θ > 20	0
–35 <= θ < -30 or 20 >= θ > 15	1
–30 <= θ < -25 or 15 >= θ > 10	2
–25 <= θ < -15 or 10 >= θ > 5	3
-15 <= θ <= 5	***4***
Wave Direction Factor =	***4***

Wave Height	
Height, Ho (ft)	Factor
Ho < 1	0
1 <= Ho < 2	0.5
2 <= Ho < 3	***1***
3 <= Ho < 5	2
5 <= Ho < 8	3
Ho >= 8	4
Wave Height Factor =	***1***

Tide	
Tide, h (m)	Factor
h > -0.2	0
- 0.5 < h <= -0.2	***1***
- 0.75 < h <= -0.5	2
h <= -0.75	1
Tidal Factor =	***1***

Directional Spreading	
Dspr, (θ°)	Factor
θ > 35	0
30 < θ <= 35	***3***
θ < 30	4
Dspr Factor =	***3***

Sum the factors: The Modified ECFL LURCS rip current threat =	***9.5***

Figure A.2: Modified ECFL LURCS checklist. A rip current warning is issued if the rip current threat is greater than 5. Very high threat would be issued at 9 or greater.

APPENDIX B
MATLAB® ROUTINES

ECFL LURCS Routine

```
function t=lurcs(Ho,T,tid,dwsp,dwdr)
%
%  Jason Engle 4/1/03
%
%  Computes the ECFL LURCS rip current threat
%
%  threat=lurcs(Ho,T,tid,dwsp,dwdr)
%
%  Ho-deep water wave height (ft)
%  T-peak wave period
%  tid-mean water level (-1 to 1)(ft)
%  dwsp-wind speed (knots)
%  dwdr-wind direction (0=shore-normal, ccw positive)
%
%The LURCS scale was configured with NDBC wave buoy data as the
% intended input for wave period and height. The Canaveral buoy is
% in 42m water depth. The use of data from a nearshore wave gage
% neccessitates that a regression be done between concurrent wave
heights
% measured at both locations so that the near shore data can be
% multiplied by a factor to compensate for a reduction in wave height
due
% to friction loss. If this is not done, the scale will under-predict
% the wave height factor.

i=find(dwdr > -35 & dwdr < 35);%wdr is 0 at shore-normal (40-110 deg
clockw. of north)
n=find(dwdr <=- 35 | dwdr >= 35);%%wdr is 0 at shore-normal (40-110 deg
clockw. of north)

Ho=Ho.*3.2808.*1.58;% 1.58 was the regression factor between the buoy
% and the gage in 14m water depth. 3.2808 converts the measurement in
% meters to feet

dwsp=dwsp*1.9438444;%convert m/s speed to knot

for j=1:length(i);
   if dwsp(i(j)) < 5
      wfact(i(j))=0;
   elseif dwsp(i(j))==5
      wfact(i(j))=.5;
   elseif dwsp(i(j)) >5 & dwsp(i(j)) < 10
      wfact(i(j))=1;
   elseif dwsp(i(j)) == 10
```

```
      wfact(i(j))=1.5;
   elseif dwsp(i(j)) >10 & dwsp(i(j)) <15
      wfact(i(j))=2;
   elseif dwsp(i(j)) == 15
      wfact(i(j))=3;
   elseif dwsp(i(j)) >15 & dwsp(i(j)) <20
      wfact(i(j))=4;
   else
      wfact(i(j))=5;
   end
end

for j=1:length(n);
   if dwsp(n(j)) <= 5
      wfact(n(j))=0;
   elseif dwsp(n(j)) >5 & dwsp(n(j)) < 10
      wfact(n(j))=.5;
   elseif dwsp(n(j)) == 10
      wfact(n(j))=1;
   elseif dwsp(n(j)) >10 & dwsp(n(j)) <15
      wfact(n(j))=1.5;
   elseif dwsp(n(j)) == 15
      wfact(n(j))=2;
   elseif dwsp(n(j)) >15 & dwsp(n(j)) <20
      wfact(n(j))=3;
   else
      wfact(n(j))=4;
   end
end

%swell height factor
for i=1:length(Ho)
   if Ho(i)<1;
      Hofact(i)=0;
   elseif Ho(i)>=1 & Ho(i)<2;
      Hofact(i)=.5;
   elseif Ho(i)>=2 & Ho(i)<3;
      Hofact(i)=1;
   elseif Ho(i)>=3 & Ho(i)<5;
      Hofact(i)=2;
   elseif Ho(i)>=5 & Ho(i)<8;
      Hofact(i)=3;
   else
      Hofact(i)=4;
   end

end

%swell period factor
for i=1:length(T)
   if T(i)<6;
      Tfact(i)=0;
   elseif T(i)>=6 & T(i)<9;
      Tfact(i)=.5;
   elseif T(i)>=9 & T(i)<11;
      Tfact(i)=1;
   elseif T(i)>=11 & T(i)<12;
```

```
      Tfact(i)=2;
   else
      Tfact(i)=3;
   end

end


%miscellaneous factor
misc(1)=0;
for i=2:length(Ho);
   if wfact(i-1)>2 | (Hofact(i-1)+Tfact(i-1))>1.5;
      miscws(i)=.5;
   else
      miscws(i)=0;
   end
      if abs(tid(i)) > .75;
      misctid(i)=.5;
   else
      misctid(i)=0;
   end
   misc(i)=miscws(i)+misctid(i);
end

t=wfact+Hofact+Tfact+misc;
```

Modified ECFL LURCS Routine

```
function threat=lmod(Ho,T,Do,tid,dspr)
%
%  Jason Engle 4/1/03
%
%threat=lmod(Ho,T,Do,tid,dspr)
%
%  Computes the modified ECFL LURCS rip current threat
%
%  Ho-deep water wave height (ft)
%  T-peak wave period
%  Do-deep water wave direction (degrees)
%     zero = shore-normal; positive ccw from shore normal
%  tid-mean water level (-1 to 1)(ft)
%  dspr-directional spreading (degrees); see Jason Engle's thesis
%     for details
%
%The LURCS scale was configured with NDBC wave buoy data as the
% intended input for wave period and height. The Canaveral buoy is
% in 42m water depth. The use of data from a nearshore wave gage
% neccessitates that a regression be done between concurrent wave
heights
% measured at both locations so that the near shore data can be
% multiplied by a factor to compensate for a reduction in wave height
due
% to friction loss. If this is not done, the scale will under-predict
% the wave height factor.

Ho=Ho.*3.2808.*1.58;% 1.58 was the regression factor between the buoy
% and the gage in 14m water depth. 3.2808 converts the measurement in
% meters to feet


for i=1:length(Ho)
   if Ho(i)<1;
      Hofact(i)=0;
   elseif Ho(i)>=1 & Ho(i)<2;
      Hofact(i)=.5;
   elseif Ho(i)>=2 & Ho(i)<3;
      Hofact(i)=1;
   elseif Ho(i)>=3 & Ho(i)<5;
      Hofact(i)=2;
   elseif Ho(i)>=5 & Ho(i)<8;
      Hofact(i)=3;
   else
      Hofact(i)=4;
   end

end

%swell period factor
for i=1:length(T)
   if T(i)<6;
      Tfact(i)=0;
   elseif T(i)>=6 & T(i)<9;
```

```
      Tfact(i)=.5;
   elseif T(i)>=9 & T(i)<11;
      Tfact(i)=1;
   elseif T(i)>=11 & T(i)<12;
      Tfact(i)=2;
   else
      Tfact(i)=3;
   end

end

%swell direction factor
for i=1:length(Do)%wave dir factor
   if Do(i)<-35 | Do(i)>20;
      Dofact(i)=0;
   elseif Do(i)<-30 | Do(i)>15;
      Dofact(i)=1;
   elseif Do(i)<-25 | Do(i)>10;
      Dofact(i)=2;
   elseif Do(i)<-15 | Do(i)>5;
      Dofact(i)=3;
   else
      Dofact(i)=4;
   end

end

%tide factor
for i=1:length(tid)%wave dir factor
   if tid(i)>0;
      tidfact(i)=0;
   elseif tid(i)>-.2 & tid(i)<=0;
      tidfact(i)=0;
   elseif tid(i)>-.5 & tid(i)<=-.2;
      tidfact(i)=1;
   elseif tid(i)>-.75 & tid(i)<=-.5;
      tidfact(i)=2;
   else
      tidfact(i)=1;
   end
end
%directional spreading factor
for i=1:length(dspr)%wave dir factor
   if dspr(i)>40;
      dsprfact(i)=0;
   elseif dspr(i)>35 & dspr(i)<=40;
      dsprfact(i)=0;
   elseif dspr(i)>30 & dspr(i)<=35;
      dsprfact(i)=3;
   else %dspr(i)<=30;
      dsprfact(i)=4;
   end
end
threat=Hofact+Dofact+tidfact+Tfact+dsprfact;
```

LIST OF REFERENCES

Bowen, A. J., *Rip currents, 1, Theoretical investigations*, J. Geophys. Res., 74(23), 5467-5478, 1969.

Brander, R. W., *Field observations on the morphodynamic evolution of a low-energy rip current system*, Marine Geo., 157(3-4), 199-217, 1999

Brander, R. W. and A. D. Short, *Flow kinematics of low-energy rip current systems*, J. of Coastal Res., 17(2), pp. 468-481, 2001.

Charles, L., R. Malakar, R.G. Dean, *Sediment data for Florida's east coast*, Report, Department of Civil and Coastal Engineering, University of Florida, 1994

Dalrymple, R. A., *Rip currents and their causes*, Proc. 16th Conf. on Coastal Eng., New York, ASCE, Vol. II, 1414-1427, 1978

Dronen, N., H. Karunarathna, J. Fredsoe, B. M. Sumer, R. Deigaard, *An experimental study of rip channel flow*, J. of Coastal Eng., 45, pp. 223-238, 2002.

Fredsoe, J., R. Deigaard, *Mechanics of coastal sediment transport*, Singapore, World Scientific Publishing Co. Pte. Ltd., pp.152, 1992

Haller, M. C., R. A. Dalrymple, I. A. Svendsen, *Rip channels and nearshore circulation*, Proc. Coastal Dynamics, Reston, Virginia, ASCE, 594-603, 1997

Johnson, D.,*DIWASP, a directional wave spectra toolbox for MATLAB®: User Manual.* Research Report WP-1601-DJ (V1.1), Centre for Water Research, University of Western Australia. 2002.

Komar, P. D., *Beach processes and sedimentation*, Upper Saddle River, New Jersey, Prentice-Hall Inc., pp.343-350, 1976

Lascody, L. L. *East central Florida rip current program*, Natl. Wea. Dig., Vol. 22, No. 2, 1998.

List, J. H., *Wave groupiness variations in the nearshore,* J. Coastal Engineering, 15, pp. 475-496, 1991.

Longuet-Higgins, M. S., D. E. Cartwright and N. D. Smith, 1963. *Observations of the directional spectrum of sea waves using the motions of a floating buoy.* J. Oceanogr. Soc. Japan, 19, 169-181.

Longuet-Higgins, M. S., and R. W. Stewart. *Radiation stress in water waves*, *A physical discussion with applications,* Deep Sea Res., 11(4), 529-563, 1964.

Longuet-Higgins, M. S., *On the joint distribution of the periods and amplitudes of sea waves,* J. of Geo. Res., 80(18), pp. 2688-2694, 1975.

Lushine, J. B., *A study of rip current drownings and related weather factors*, Natl. Wea. Dig., Vol. 16, 1991.

MacMahan, J., R. J. Thieke, R. G. Dean, D.M. Hanes, and R.A. Holman. *Rip currents at Duck, NC: Hydraulically efficient flows through relict caps in a longshore bar*. EOS Transactions, San Francisco, 2000.

MacMahan, J., A.J.H.M. Reniers, T.P. Stanton, and E.B. Thornton, *Infragravity motions on a complex beach, part 1: Observations.* Submitted to J. of Geophys. Res., Dec., 2003.

McKenzie, P., *Rip current systems*, J. of Geology, 66(2), pp. 103-113, 1958.

Mei, C. C. and P. L-F. Lui, *Effects of topography on the circulation in and near the surf zone-linear theory*, J. Estuary Coastal Mar. Sci., 5, 25-37, 1977

National Data Buoy Center, *Station 41009 historical data, 1996*, NOAA/NDBC, Available [on-line], accessed 10/5/02, http://seaboard.ndbc.noaa.gov/station_history?$station=41009

Oh, T. M. and R. G. Dean, *Three-Dimensional Hydrodynamics on a Barred Beach*, Proc. Intl. Conf. Coastal Eng., New York, ASCE, 3680-3692, 1996.

Pawka, S. S., *Wave directional characteristics on a partially sheltered coast.* Ph.D. dissertation, University of California, San Diego, 249 pp., 1982.

Shepard, F. P., K. O. Emery, and E. C. LaFond, *Rip currents: A process of geological importance*, J. Geol., 49(4), 337-369, 1941.

Shepard, F. P., and D. L. Inman, *Nearshore water circulation related to bottom topography and wave refraction*, Eos Trans. AGU, 31(2), 196-212, 1950.

Short, A. D., *Rip current type spacing and persistence narrabeen beach, Australia*, J. Mar. Geology, 65, pp. 47-71, 1985.

Short, A. D. and C. L. Hogan, *Rip currents and beach hazards: Their impact on public safety and implication for coastal management*, J. of Coastal Res. Special Issue No. 12: Coastal Hazards, pp. 197-209, 1993.

Sonu, C. J., *Field observations of nearshore circulation and meandering currents*, J. Geophys. Res., 77, 3232-3247, 1972.

U.S. Army Corps of Engineers Waterways Experiment Station, *Coastal inlet research program (CIRP) long term measurement program*, 1995, Available [on-line], accessed 9/23/02, http://sandbar.wes.army.mil/public_html/pmab2web/htdocs/projects/proj_cirp.html

Volusia County Council, *Volusia County, Florida Beach Patrol*, pamphlet, Daytona Beach, 2003

BIOGRAPHICAL SKETCH

Jason Engle was born in Marquette, Michigan, on May 19, 1970. Growing up on Lake Michigan's beaches instilled a lifelong love of the water; a move to Florida at age 15 only reinforced this passion. After graduating from high school in 1988, he attended St. Petersburg College in Clearwater, Florida, for general education and was accepted to Florida Atlantic University Department of Ocean Engineering in 1990. In 1991 he decided to leave school and soon found an apprenticeship at a well-known local glass-art studio run by Robin Saenger. There he mastered stained and carved glass construction and design. By 1997 Jason was engaged to Jennifer Oppegard who was finishing her two-year degree at St. Petersburg College. At this point, the art-glass position reached a natural stopping point and Jason was ready to finish his degree (much to his parents' delight).

In 1998 the couple moved to Gainesville, FL, and in the summer of 2000 they were married. Both Jason and Jennifer graduated with bachelor's degrees in spring 2001. The last several semesters of Jason's undergraduate degree were spent working in the coastal engineering program with Dr. Robert Thieke (assistant professor) and Jamie MacMahan (graduate student) on various parts of a rip current project including video image analysis, rip current rescue analysis and construction of a personal watercraft-mounted bathymetric survey system. That research lead to admission into the Coastal and Oceanographic Engineering program at UF. The fulfillment of this Master of Science degree will ensure that home will always be near the beach.